AD-A112 209 NAVAL OCEAN SYSTEMS CENTER SAN DIEGO CA F/G 17/4
EHF MULTIPLE BEAM ANTENNAS.(U)
SEP 81 R W MAJOR, J M DEVAN
UNCLASSIFIED NOSC/TR-730 NL

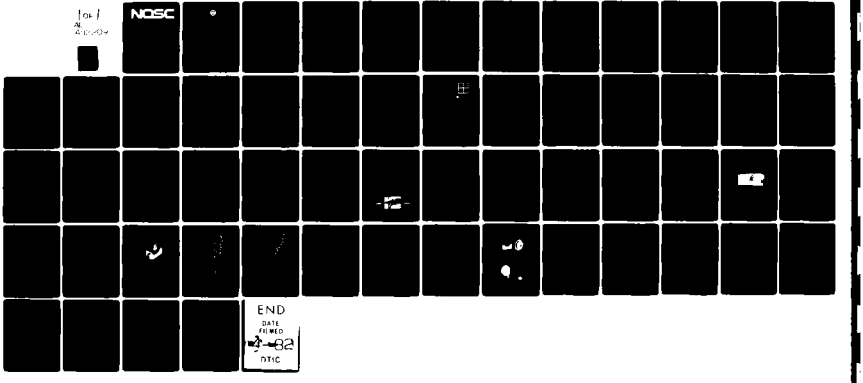

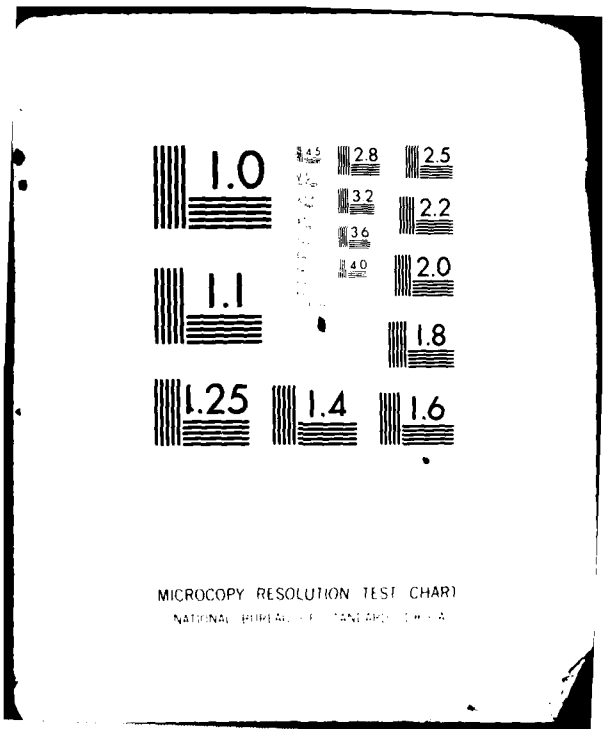
1.0
1.1
1.25
1.4
1.6
1.8
2.0
2.2
2.5
2.8
3.2
3.6
4.0
MICROCOPY RESOLUTION TEST CHART

(12)

NOSC

NOSC TR 730

NOSC TR 730

ADA112209

Technical Report 730

ehf MULTIPLE BEAM ANTENNAS

R.W. Major
J.M. Devan

21 September 1981

Produced for
NOSC IR/IED Program

Approved for public release; distribution unlimited

NAVAL OCEAN SYSTEMS CENTER
SAN DIEGO, CALIFORNIA 92152

NAVAL OCEAN SYSTEMS CENTER, SAN DIEGO, CA 92152

AN ACTIVITY OF THE NAVAL MATERIAL COMMAND

SL GUILLE, CAPT, USN
Commander

HL BLOOD
Technical Director

ADMINISTRATIVE INFORMATION

This report summarizes work performed during the period November 1979–October 1981. This effort was performed with NOSC IED funding under program element 62766N, project F66212, task ZF66212001, and work unit 811-ZD70.

Released by
M. S. Kvigne, Head
Communications Research and
Technology Division

Under authority of
H. D. Smith, Head
Communications Systems
and Technology Department

ACKNOWLEDGMENT

The investigators wish to acknowledge and thank A. R. Hislop and D. L. Saul, Code 9262, for their work on the mixer design and D. L. Chappelle and K. S. Maynard, Code 8124, for their work on measuring system performance. Special thanks are due K. R. Casey, Code 8143, whose inspiration and constant support helped make this effort possible.

METRIC CONVERSION

1 inch (1") = 25.4 mm

UNCLASSIFIED

SECURITY CLASSIFICATION OF THIS PAGE *(When Data Entered)*

REPORT DOCUMENTATION PAGE		READ INSTRUCTIONS BEFORE COMPLETING FORM
1. REPORT NUMBER NOSC Technical Report 730 (TR 730)	2. GOVT ACCESSION NO. AD-A112269	3. RECIPIENT'S CATALOG NUMBER
4. TITLE *(and Subtitle)* ehf MULTIPLE BEAM ANTENNAS		5. TYPE OF REPORT & PERIOD COVERED Final November 1979–October 1981
		6. PERFORMING ORG. REPORT NUMBER
7. AUTHOR(s) R. W. Major J. M. Devan		8. CONTRACT OR GRANT NUMBER(s)
9. PERFORMING ORGANIZATION NAME AND ADDRESS Naval Ocean Systems Center San Diego CA 92152		10. PROGRAM ELEMENT, PROJECT, TASK AREA & WORK UNIT NUMBERS 62766N, F66212, ZF 66212001, 811-ZD070
11. CONTROLLING OFFICE NAME AND ADDRESS		12. REPORT DATE 21 September 1981
		13. NUMBER OF PAGES 56
14. MONITORING AGENCY NAME & ADDRESS *(if different from Controlling Office)*		15. SECURITY CLASS. *(of this report)* Unclassified
		15a. DECLASSIFICATION/DOWNGRADING SCHEDULE

16. DISTRIBUTION STATEMENT *(of this Report)*

Approved for public release; distribution unlimited

17. DISTRIBUTION STATEMENT *(of the abstract entered in Block 20, if different from Report)*

18. SUPPLEMENTARY NOTES

19. KEY WORDS *(Continue on reverse side if necessary and identify by block number)*

Satellite communications
Antennas
Extreme high frequency (ehf)
Multiple beams
Antijamming

20. ABSTRACT *(Continue on reverse side if necessary and identify by block number)*

The objective of this task was to design, build, and test a multiple-beam, ehf, satellite antenna system for reception of shipboard SATCOM transmissions. The system was to provide full earth coverage with multiple spot beams. The spot beams serve to enhance gain to signals in a given sector while decreasing gain to jammers not in that sector. The chosen design was a system employing a waveguide lens and 37 feed horns. Computer simulation of a lens design indicated that the system could provide 37 simultaneous beams with a minimum gain of 27 dB over the earth, at least 40.0% efficiency, and sidelobes 20 dB down. A waveguide lens, feed horns, a mixer, and an IF amplifier were fabricated or purchased. The system provided a minimum gain of 27.4 dB, the largest sidelobe was 19.8 dB down, and efficiency ranged from 41.6 to 43.5%.

DD FORM 1 JAN 73 1473 EDITION OF 1 NOV 65 IS OBSOLETE

S/N 0102-LF-014-6601

UNCLASSIFIED

SECURITY CLASSIFICATION OF THIS PAGE *(When Data Entered)*

PROBLEM

Design, build, and test a multiple-beam, ehf, satellite antenna system for reception of shipboard SATCOM transmissions, providing full earth coverage with multiple spot beams that serve to enhance gain to signals in a given sector while decreasing gain to jammers not in that sector.

RESULTS

The chosen design was a system employing a waveguide lens and 37 feed horns. Computer simulation of a lens design indicated that the system could provide 37 simultaneous beams with a minimum gain of 27 dB over the earth, at least 40.0% efficiency, and sidelobes 20 dB down. A waveguide lens, feed horns, a mixer, and an IF amplifier were fabricated or purchased. The system provided a minimum gain of 27.4 dB, the largest sidelobe was 19.8 dB down, and efficiency ranged from 41.6 to 43.5%.

CONTENTS

FIGURES

TABLES

SYMBOLS

Waveguide element length . . . z
Refractive index . . . υ
1/1000 inch (0.0254 mm) . . . mil
Aperture size (diameter) . . . D
Focal length . . . F
Horn diameter and spacing . . . d
Inner dimension of waveguide . . . a
Waveguide wall thickness . . . τ
Bandwidth . . . bw
Beamwidth . . . BW
Efficiency . . . η
Azimuth angle . . . ϕ
Angle from nadir . . . θ
Peak gain . . . G_p
Minimum gain . . . G_{min}
Conversion loss . . . L_c
Noise figure . . . NF
Local oscillator . . . LO
Radio frequency . . . rf
Intermediate frequency . . . IF
Probability of system success . . . P_s
Probability of beam success . . . P_B
1/MTTF for diode and IF amp . . . λ_D and λ_{IF}
Mean time to failure . . . MTTF

1.0 INTRODUCTION

This report presents information regarding the design, fabrication, and test of a satellite antenna system for the reception of shipboard ehf SATCOM transmissions. To provide full earth coverage, the antenna on a synchronous-orbit satellite needs only one beam with a beamwidth of 17.3° or greater. The design presented here, however, will attempt to provide the same coverage with multiple spot beams, as depicted in figure 1. The spot beams will enhance gain to signals from a given sector of the earth while discriminating against signals (jammers) from other earth sectors. The antenna design goals are as follows:

Frequency	43–45 GHz
Beamwidth	3° or less
Scan coverage	17.3°
Polarization	Circular
Aperture size	<25 cm (10 inches)
Reception	All beams simultaneously.

Since antennas employing rf lenses have the capability of providing this kind of performance, several types of such lenses are considered in section 2. Section 3 discusses the chosen lens design and its predicted performance. Section 4 presents the design of the mixers required by this system. Section 5 discusses system fabrication and test.

2.0 LENS TYPES

There are several types of lenses capable of producing multiple spot beams. A representative group of lenses which were considered for this application are discussed below:

a. Luneberg lens – a spherically symmetric, dielectric lens. It is aberration-free and reflection-free. Its spherical symmetry gives it an unlimited scan capability. The refractive index varies from the center to the edge of the sphere ($\upsilon = \sqrt{2 - (r/a)^2}$, where a is the radius at the edge). Approximation of this is difficult at best and probably impractical above 10 to 20 GHz.

b. R – 2R lens – a bootlace lens typically formed as shown in figure 2a. There is no aberration with this lens when scanning ±50° or less. This lens requires equal-length constrained paths between the two radii and thus tends to be impractical above 18 GHz, where the use of coax cable is impractical.

c. Rotman lens – a bootlace lens typically formed as shown in figure 2b. It is capable of large scan angles and its scan characteristics are essentially frequency-independent. This lens requires constrained paths of specific lengths (the center paths being the longest, the edge paths the shortest) between the outer radius and the excited elements. As with the R – 2R lens, this is impractical above about 18 GHz.

d. Spherical constant –υ lens – a spherically symmetric, dielectric lens whose refractive index is constant (between 1.5 and 1.8). Like the Luneberg lens, it has an unlimited scan potential but it does suffer from surface reflections (which can be eliminated with quarter-wave matching layers) and even-order aberrations which limit its diameter to less than 125 wavelengths.

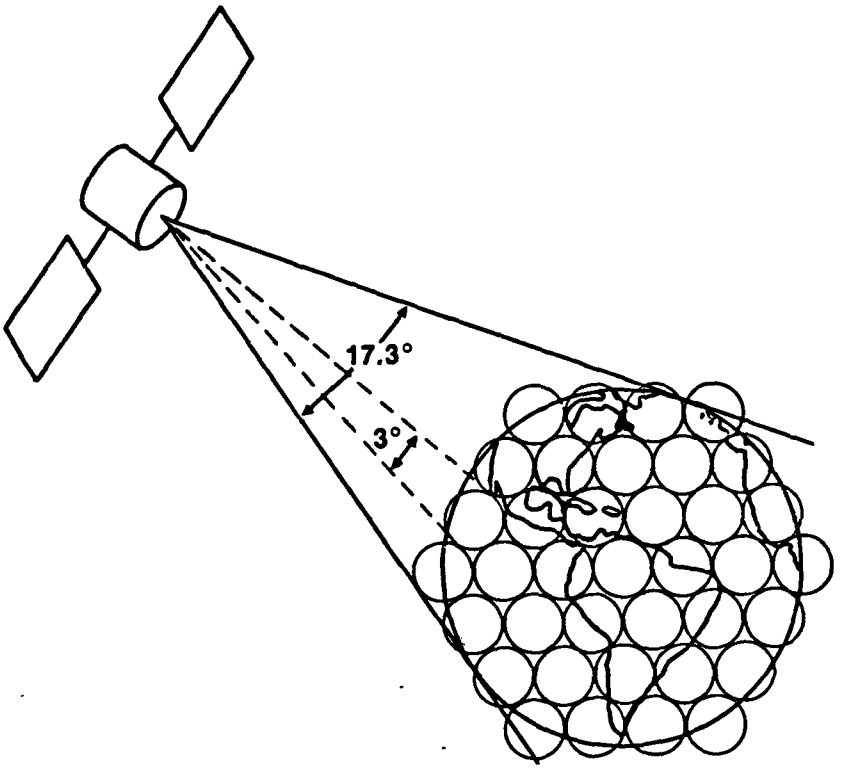

Figure 1. Full earth coverage.

e. Waveguide lens -- a lens consisting of a 2-dimensional array of waveguide sections stacked parallel to the lens axes. These lenses are capable of large scan angles ($37° \times$ [beamwidth]$^{1/3}$). They are, however, narrow bandwidth devices (typically >5% for zoned lenses) and at 44 GHz have very small construction tolerances (on the order of 5 mils).

Since the desired operating frequency is 44 GHz with a bandwidth of less than 5%, two of the lens types are applicable: the spherical constant $-\nu$ lens and the waveguide lens.

The constant $-\upsilon$ spherical lens design is depicted in figure 3. Polystyrene was chosen as the dielectric. Its refractive index is 1.59 and its loss tangent 7.21×10^{-4} [ref 1]. For a beamwidth of 3° or less, the lens diameter must be at least 9 inches and its weight will be at least 15 pounds. The dielectric loss is represented by

$$L_d = 8.686 \frac{\pi}{\lambda} \tan \delta \, \upsilon \, 2a$$

giving $L_d = 1.04$ dB for this design [ref 2]. The concern is that thermal expansion may be a problem for the dielectric in the satellite environment (possibly breaking the sphere or altering its refractive index).

---

1. Balanis, C.A., Dielectric Constant and Loss Tangent Measurement at 60 and 90 GHz Using the Fabry-Perot Interferometer, Microwave Journal, p 39-44, March 1971.
2. Saad, T.S., Microwave Engineer's Handbook, v 1, p 15, Artech House, Inc, 1971.

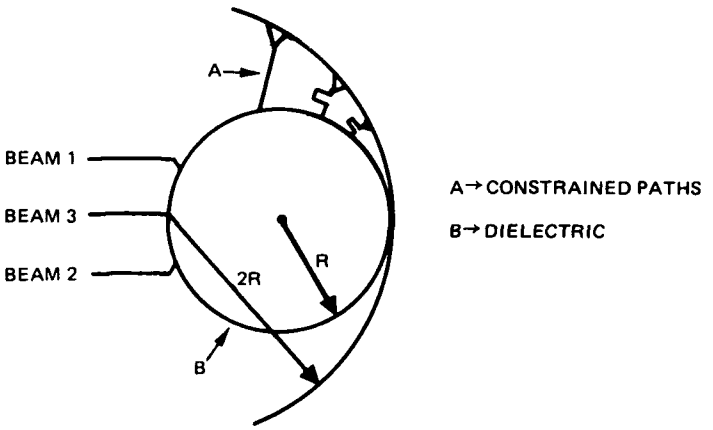

(a) R-2R Lens

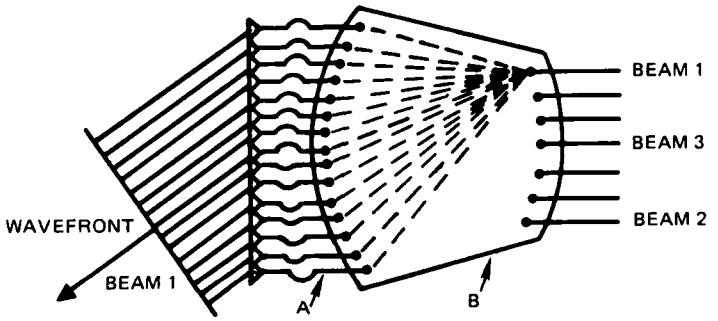

(b) Rotman Lens

Figure 2. R – 2R and Rotman lenses.

The waveguide lens design is shown in figure 4. The lens should be designed such that it creates a plane wave. This assumes that the time delay for each path through the lens to the focal point will be equal. Thus, from figure 4, the time delay for the 0 – 2 path ($F/C + Z_2/C$) must equal the delay for the 0 – 3 – 1 path ($\rho/C + Z_0/C/\upsilon$); C/υ being the velocity through the waveguide element where υ is the refractive index. Refractive index is given by $\upsilon = \sqrt{1 - (\lambda/2a)^2}$ where λ is the free-space wavelength and a is the inner dimension of the waveguide. Since a is restricted to between 0.5λ and λ, υ will be between 0 and 0.866, with 0.5 considered the minimum practical value. Since the coordinates at point 0 are (0,0,–F) and at point 3 are (X,Y,Z_1),

$$\rho = \sqrt{(X-0)^2 + (Y-0)^2 + (Z_1 + F)^2}$$

and

$$\frac{F + Z_2}{C} = \frac{\sqrt{X^2 + Y^2 + (Z_1 + F)^2}}{C} + \frac{Z_0}{C/\upsilon} .$$

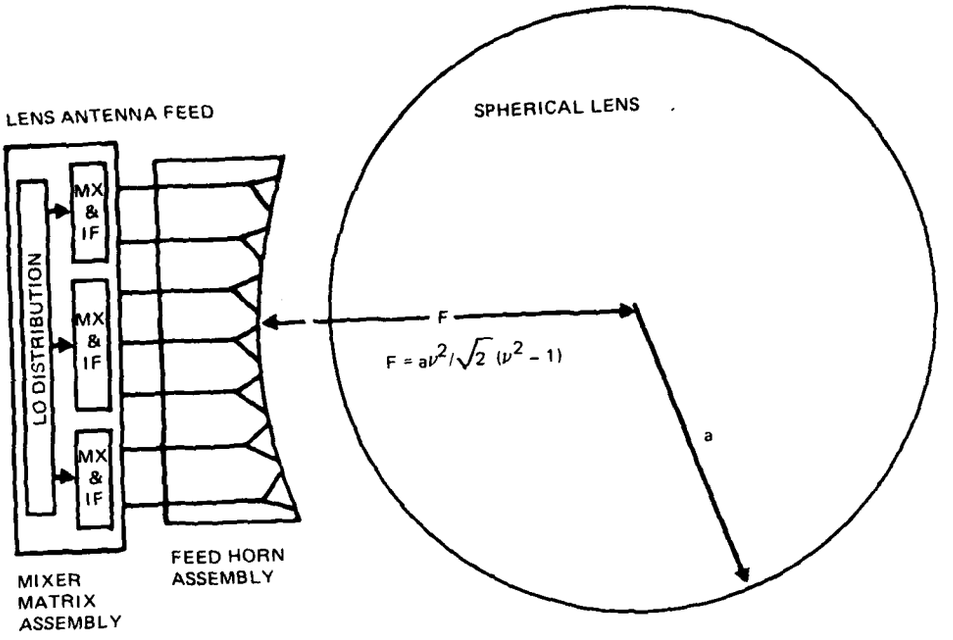

Figure 3. Constant $-\upsilon$ spherical lens system.

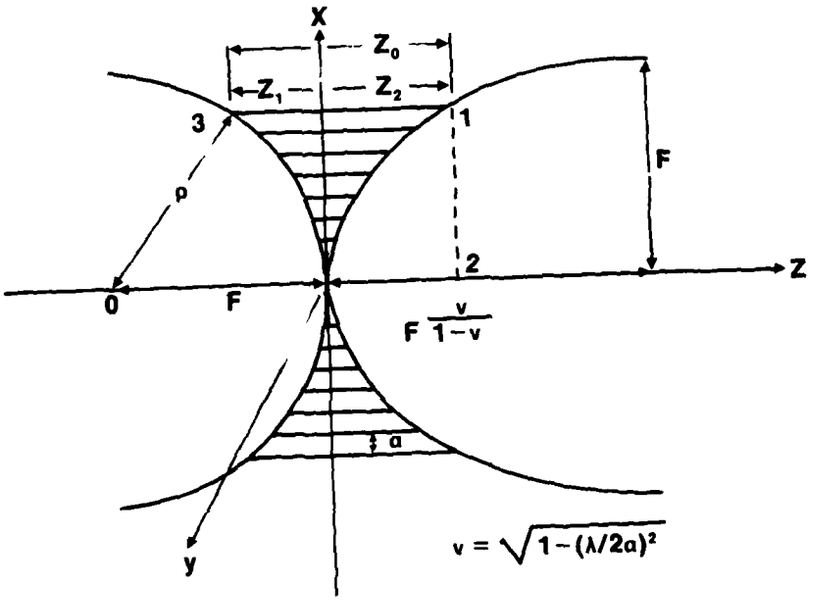

Figure 4. Waveguide lens.

Canceling the Cs and setting $Z_0 = Z_2 - Z_1$ (Z_1 is negative),

$$F + Z_2 = \sqrt{X^2 + Y^2 + (Z_1 + F)^2} + (Z_2 - Z_1)v$$

or

$$Z_2 - Z_2 v = \sqrt{X^2 + Y^2 + (Z_1 + F)^2} - F - Z_1 v .$$

By setting the inner surface of the lens equal to a sphere of revolutions of radius F centered at $-F$, $X^2 + Y^2 + (Z_1 + F)^2 = F^2$, Z_1 can be derived as $Z_1 = \sqrt{F^2 - X^2 - Y^2} - F$. Substituting this into the equation for Z_2 yields

$$Z_2(1 - v) = \sqrt{X^2 + Y^2 + (\sqrt{F^2 - X^2 - Y^2} - F + F)^2} - F - Z_1 v$$

or

$$Z_2(1 - v) = F - F - Z_1 v = (F - \sqrt{F^2 - X^2 - Y^2})v .$$

This equation can be rewritten in the form

$$\frac{X^2}{F^2} + \frac{Y^2}{F^2} + \frac{\left[Z_2 - F\frac{v}{1-v}\right]^2}{F^2\left[\frac{v}{1-v}\right]^2} = 1$$

which shows that the outer surface of the lens is an ellipsoid of revolution centered at $(0, 0, F\frac{v}{1-v})$ and having a semimajor axis of $F\frac{v}{1-v}$ and a semiminor axis of F.

For a beamwidth of 3° or less, the lens diameter must be at least 5.4 inches ($D \approx 60\frac{\lambda}{BW}$). The weight is expected to be between 1 and 2 pounds.

Since the waveguide lens will be smaller, lighter, and more durable than the spherical dielectric lens, it was chosen for this design. Any advantage that the dielectric lens might have due to its larger size (such as better efficiency due to greater illumination taper) will probably be negated by its dielectric loss (L_d).

3.0 CHOSEN LENS DESIGN

The lens design must be capable of covering the surface of the earth with 37 beams, as shown in figure 5a. To achieve this, a horn antenna configuration (figure 5b) must be mounted behind the lens. The problem is to configure the lens and horns so as to maximize the minimum gain to any point on the earth. Minimum gain occurs at the earth's edge (taken here as θ=9°) at points A on figure 5a, or every 60° in azimuth (ϕ). This gain can be optimized for any beamwidths (and thus any diameter since $BW \approx 60\frac{\lambda}{D}$) by choosing the beam center positions such that the gain at the crossover point of beams 55, 56, and 65 is

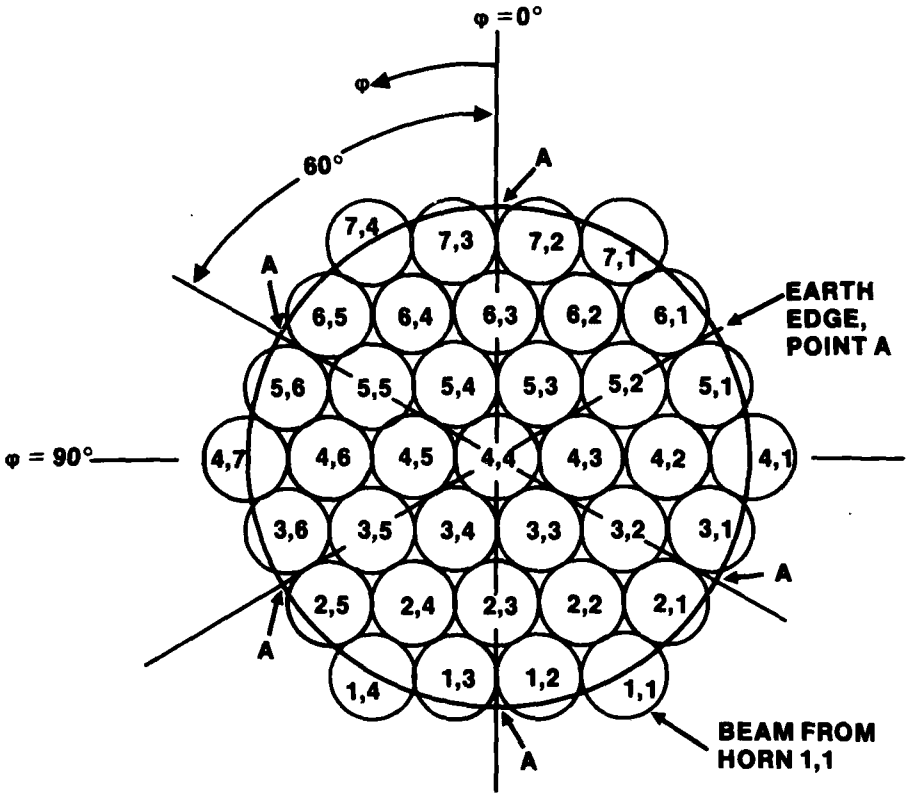

Figure 5a. Desired beam pattern on earth.

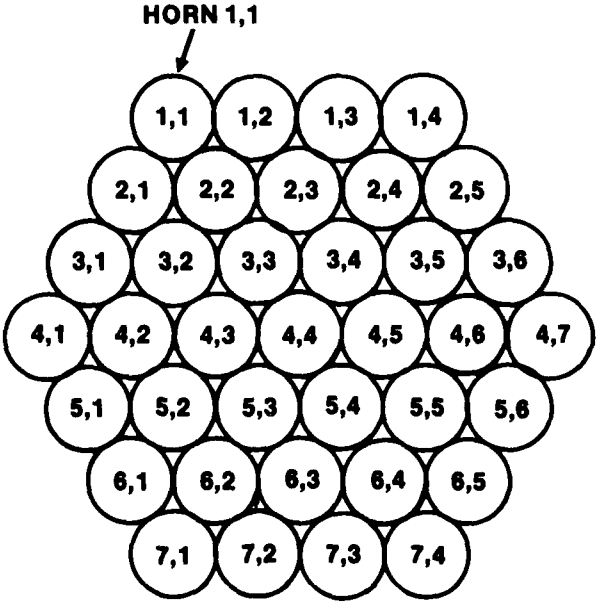

Figure 5b. Horn configuration necessary for desired beam pattern.

equal to the gain at the earth edge points A. Figure 6 shows the minimum gain for various diameter lenses as derived from computer program [ref 3a] calculations. From reference 3b the optimum G_{MIN} should occur at $D = 0.57N_c\lambda\,(1-3N_c^{-1})/\theta_m$ when θ_m is the angle at the minimum gain point (9°), N_c is the number of horn columns (7), and λ is the free-space wavelength. This yields a value of D = 6.55 inches. Figure 6 shows an optimum G_{MIN} point in good agreement with this value. It also shows that the optimum G_{MIN} curve rises with increasing υ and that the curve is fairly flat over a wide range of diameters (G_{MIN} varying less than 0.1 dB between 6- and 7-inch diameters where $\upsilon = 0.74$). The figure also shows the mainbeam efficiency at each gain/diameter point. Since an efficiency of at least 40% was desired, the diameter chosen for this lens design was the one closest to the optimum diameter that had an efficiency of at least 40%; ie, 6.9 inches.

As indicated above, there is an optimal set of beam center positions (θ_r) for any diameter lens and horn configuration. For this design, it was found that the beam centers should be spaced every 3.15° along the horizontal axis ($\phi = 90°$). From figure 7, it is seen that a beam center occurs at θ_r when a horn is displaced in the direction transverse to the focal axis by a distance d equal to $F\theta_r$ (F being the focal length). Thus, to create the desired beam patterns, the horn diameters in figure 5b must equal d and d/F must equal 0.055 radian (3.15°). Thus d/F is fixed and any increase in the ratio F/D must be accompanied by an increase in d (D being fixed). Increasing F/D decreases the number of zones in the lens. [A zone occurs where the difference in the waveguide element length in waveguide wavelengths and in free-space wavelengths $(\frac{z_0}{\lambda/\upsilon} - \frac{z_0}{\lambda})$ is an integer; ie, $Z_0 = \frac{n\lambda}{\upsilon-1}$. The implication is that each waveguide element longer than $\frac{n\lambda}{\upsilon-1}$ can be reduced in length by $\frac{n\lambda}{\upsilon-1}$ without changing the phase shift caused by the element.] Since the bandwidth of a lens is given by

$$b_w = 25\upsilon/(1 + k\upsilon)$$

where k is the number of zones [ref 4], increasing F/D increases the lens bandwidth. The increase in horn diameter accompanying the increase in F/D decreases the horn beamwidth, thus increasing the illumination taper on the lens. This results in greater efficiency, lower sidelobes, broader lens beamwidths, and lower lens gain. Figure 8 shows F/D versus efficiency as derived from computer simulation. Note that the greatest efficiency at the largest G_{MIN} occurs at F/D = 1.581. Since the chosen diameter is 6.9 inches and F/D = 1.581, F = 10.91 inches and d = 0.6 inches.

It was noted from figure 6 that, to maximize G_{MIN}, υ should be as large as practical and thus a should be as large as practical. For a waveguide lens $0.5\lambda < a < \lambda$; but to prevent grating lobes

$$a + \tau \leqslant \lambda/(1 + \sin\theta_s)$$

3a. MIT Lincoln Lab TN 1975-39, Optimization of a Communication Satellite Multiple Beam Antenna, by A.R. Dion, 17 May 1975.

3b. MIT Lincoln Lab TN 1979-33, Minimum Directive Gain of Hopped-Beam Antennas, by A.R. Dion, p 14, 11 June 1979.

4. Silver, S., Microwave Antenna Theory and Design, 1st ed, p 407 and 409, McGraw-Hill, 1949.

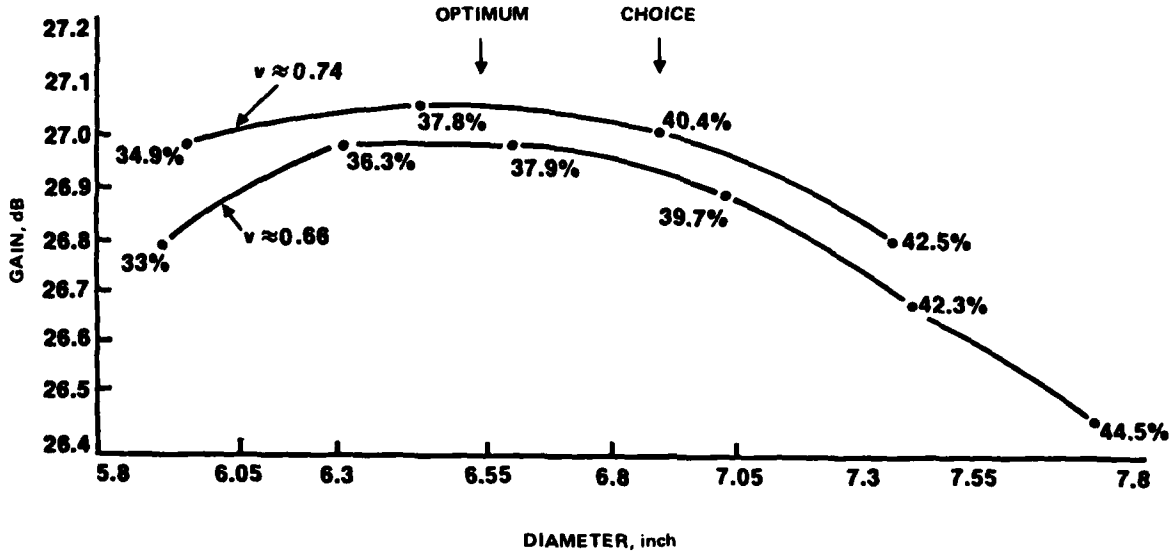

Figure 6. Minimum gain with F/D = 1.5.

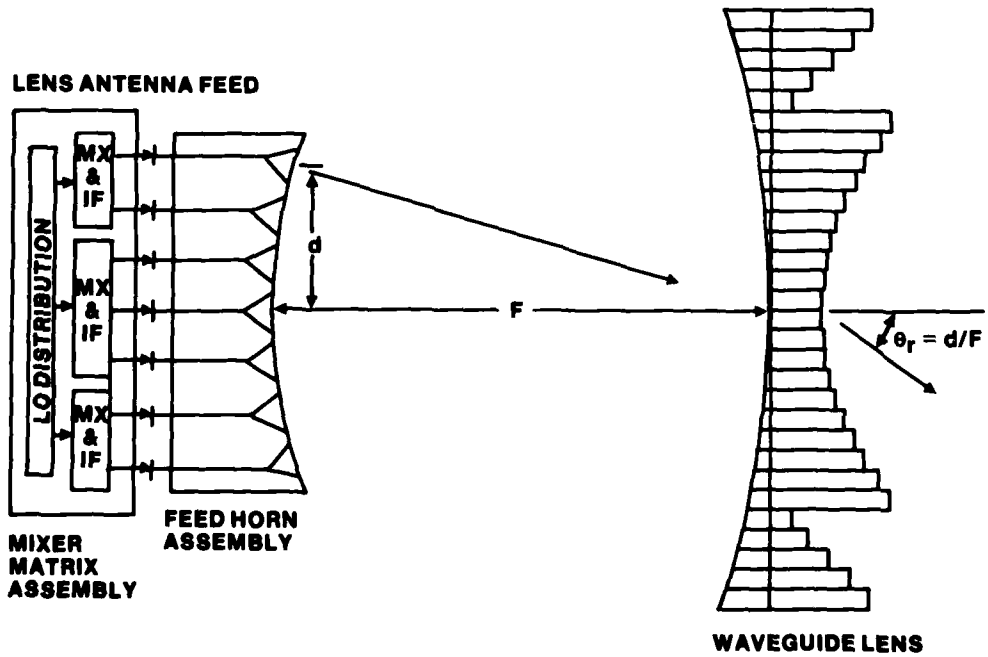

Figure 7. Multiple beam ehf satellite antenna.

where θ_s is the maximum scan angle and τ is the wall thickness. From figure 5b and θ_r = 3.15°, θ_s = 3(3.15°) = 9.45° and a + $\tau \leq$ 0.232 inch. The practical minimum value for τ is 20 mils. This gives a $\leq$ 0.212. The chosen value for a was 0.21 inch.

The chosen lens design is as follows:

D = 6.9 inches
F = 10.91 inches
d = 0.6 inch
a = 0.21 inch
τ = 0.02 inch
υ = 0.766
Bandwidth = 5.8%.

Figure 9 shows this lens design. Construction tolerances are given by

$$\Delta Z = \lambda/16(1 - \upsilon)$$

and

$$\Delta a = a\upsilon/16(1 + \upsilon)$$

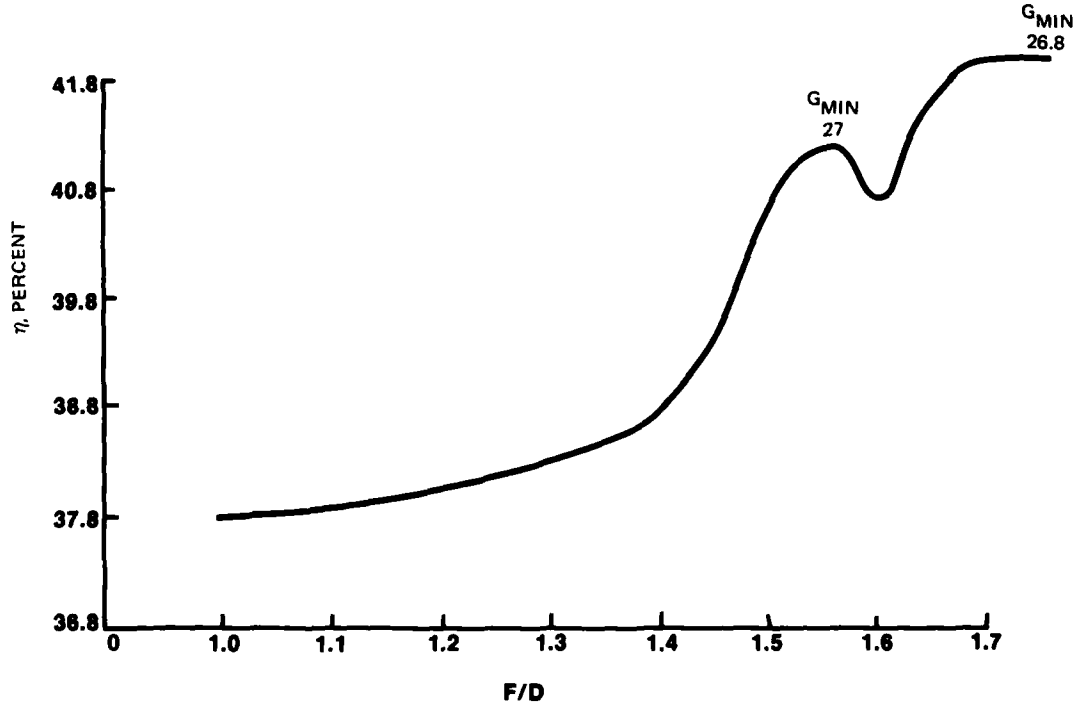

Figure 8. F/D versus efficiency.

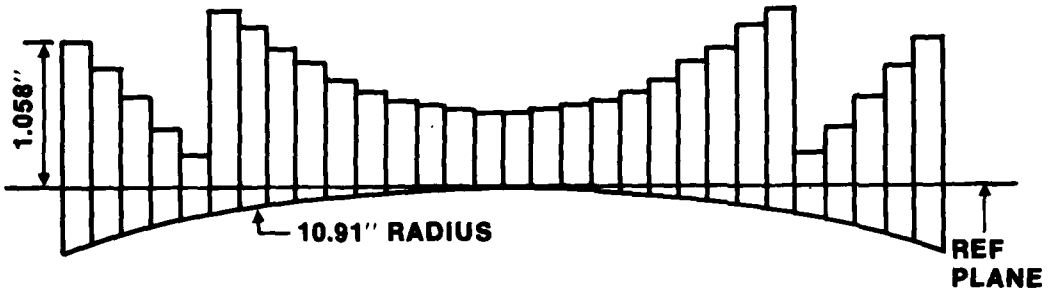

Figure 9a. Principal plane cross section.

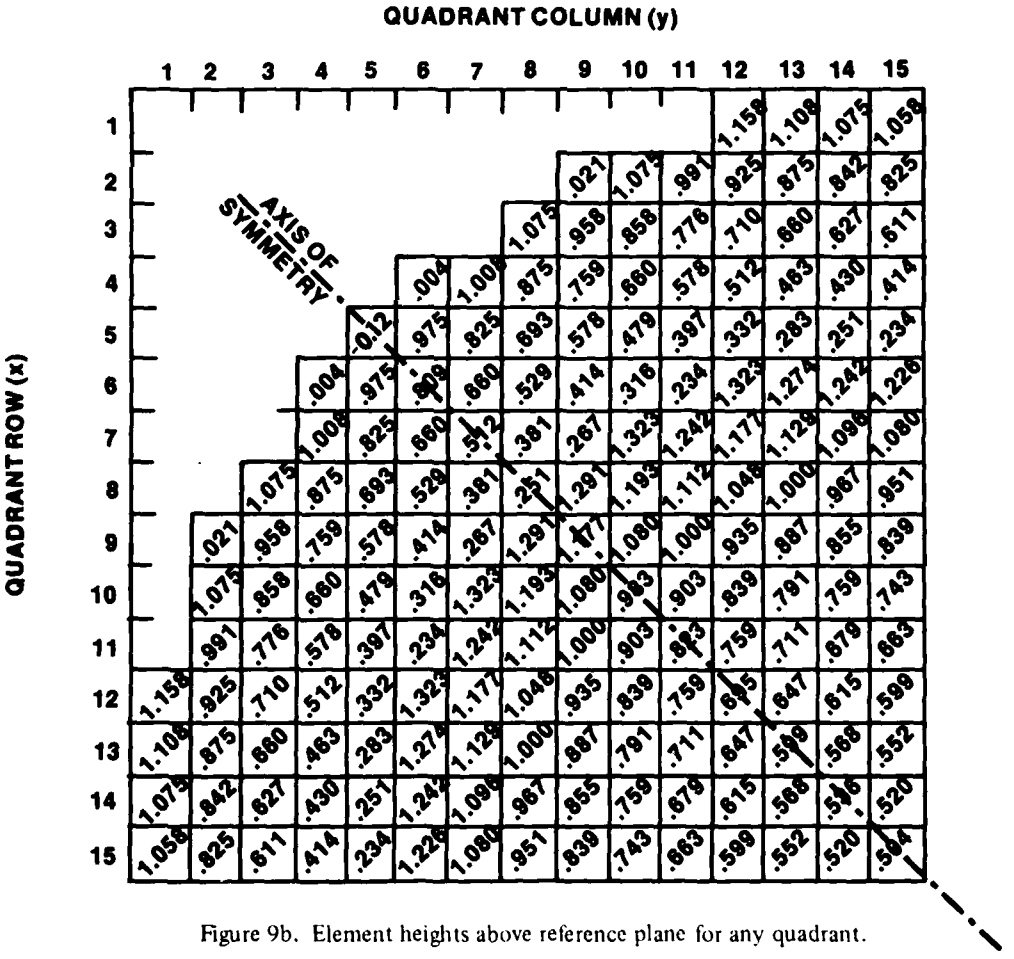

Figure 9b. Element heights above reference plane for any quadrant.

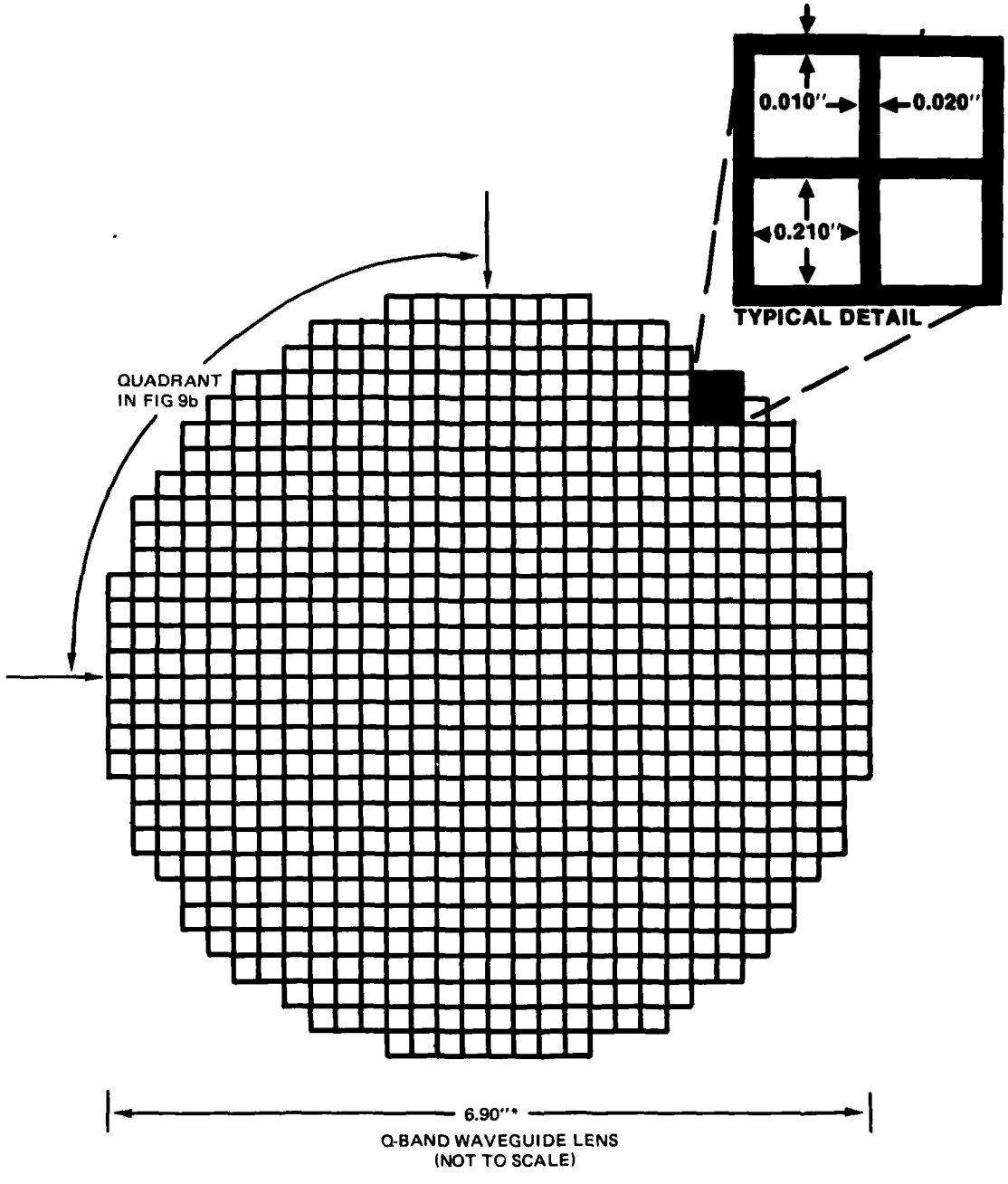

Figure 9c. Front view of lens.

Figures 10, 11, and 12 show the beam patterns that are predicted for this lens design. Figure 10a shows beams 44, 45, 46, and 47 at a 90° azimuth cut (see figure 5a), with the frequency being the design frequency for the lens: 44 GHz. Figure 10b shows beams 44, 45, 55, and 56 at a 60° azimuth cut, so that they pass through the minimum gain point A. (Note that the gain at the 55 and 56 beam crossover point is equal to that at point A, as was desired). Figures 11 and 12 show the corresponding beam patterns at the lower and upper edges of the frequency band, 43 and 45 GHz. The peak gain (G_p) and beamwidth change across the frequency band since the refractive index (υ) changes with frequency, but the values of minimum gain, efficiency, and sidelobe level are maintained across the band as:

$G_{MIN} = 27$ dB

$\eta \geqslant 40\%$

Sidelobes $\geqslant$ 20 dB down.

3.1 LOSS OF BEAM CONSIDERATION

A prime concern with a multiple beam system is the loss of coverage resulting from a loss of any beam. Thus the possibility of combining remaining beams in case of a single beam loss was considered. When summing two adjacent beams, as shown in figure 13, the resultant beam is centered about the beam crossover point with approximately 3 dB more gain than either single beam at this point. When a single beam is lost and its two adjacent beams are summed, the same effect occurs. For the loss of beam case, however, the crossover point is after the first null of the single beams and thus the combined beam provides no significant improvement in coverage. This condition is shown in figure 14, where the combined beam does show about 3 dB improvement at the crossover point of $\theta = 0°$ (from ~ 2.5 dB to ~ 5.5 dB), but shows less coverage overall than the noncombined beams. For this system, then, beam summing is obviously not the answer to the beam loss problem.

The possibility of increasing horn size by dividing the horns between two lenses was also considered, the idea being that greater horn size would cause greater illumination taper and thus greater main beam efficiency. Figure 15 depicts these considerations. The first consideration was to use every other horn in the current triangular lattice design to excite a second lens. Every shaded horn in figure 15a would form a cluster for the second lens. This, however, would allow for no increase in the size of the horns. The second consideration was of an odd square lattice (figure 15b). Here, the removal of every other element would allow each horn to expand in diameter by the factor $\sqrt{2}$. This arrangement, however, covers less of the surface area (~75% as compared with 92% for the triangular lattice). Thus a greater efficiency is achieved at the expense of a smaller G_{MIN} applied to a greater percentage of the surface area. The even square lattice of figure 15c was next considered. It can cover more of the surface area (~81%) with fewer horns than the odd square lattice and still allow for an increase in horn size. The final consideration was of an odd-plus-even square lattice shown in figure 15d. This arrangement requires 45 horns but covers the full surface area. The horn size is constrained by $d/F = 3.6°$, thus allowing for larger horns than the triangular lattice where $d/F = 3.15°$. The three candidate configurations are as follows: (1) triangular-lattice, one lens; (2) even-square lattice, two lenses; (3) odd-plus-even-square lattice, two lenses. Table 1 compares the three configurations. As can be seen, the odd-plus-even-square lattice provides slightly better G_{MIN} (~0.5 dB) and slightly better efficiency (~0.9%) than the triangular lattice but requires eight more horns and one more lens. (Note, however, that by dropping the outer eight beams, only coverage to the shaded areas of figure 15d would be lost). The advantages of a two-lens system were thus considered quite small.

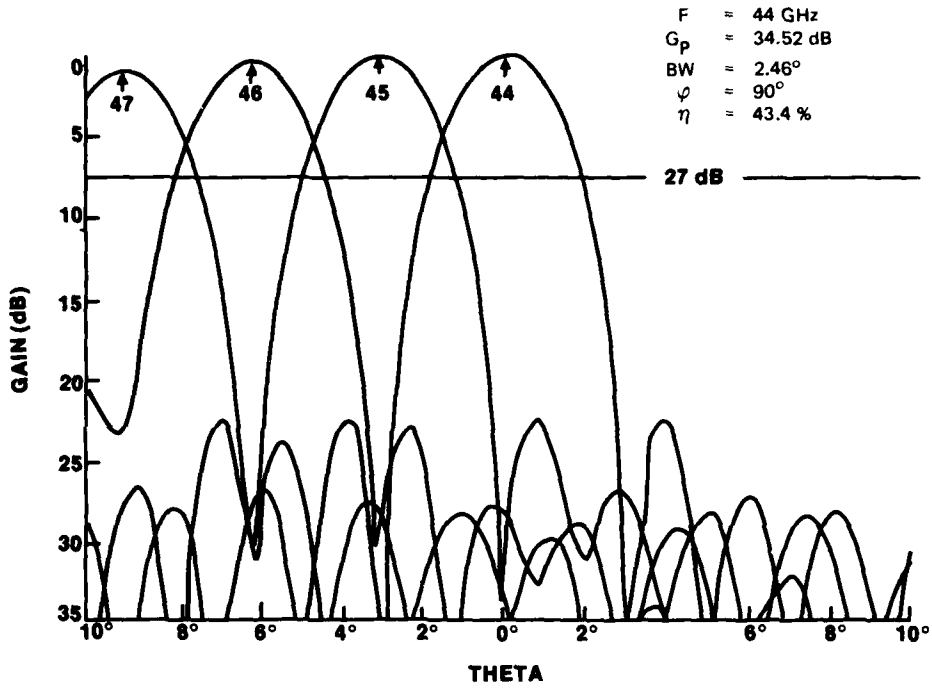

Figure 10a. Predicted lens patterns. (44 GHz, $\phi = 90°$.)

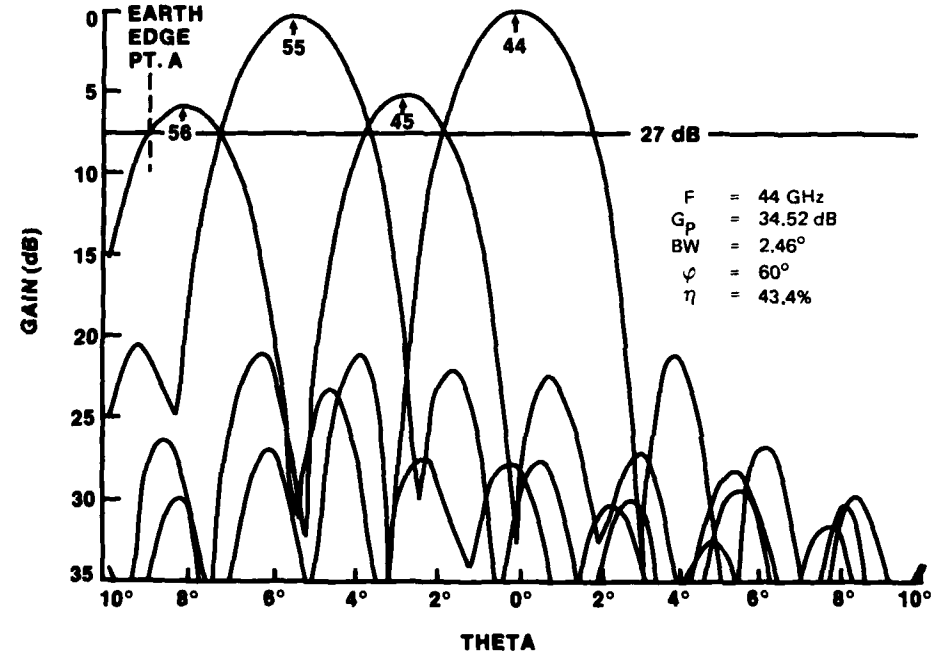

Figure 10b. Predicted lens patterns. (44 GHz, $\phi = 60°$.)

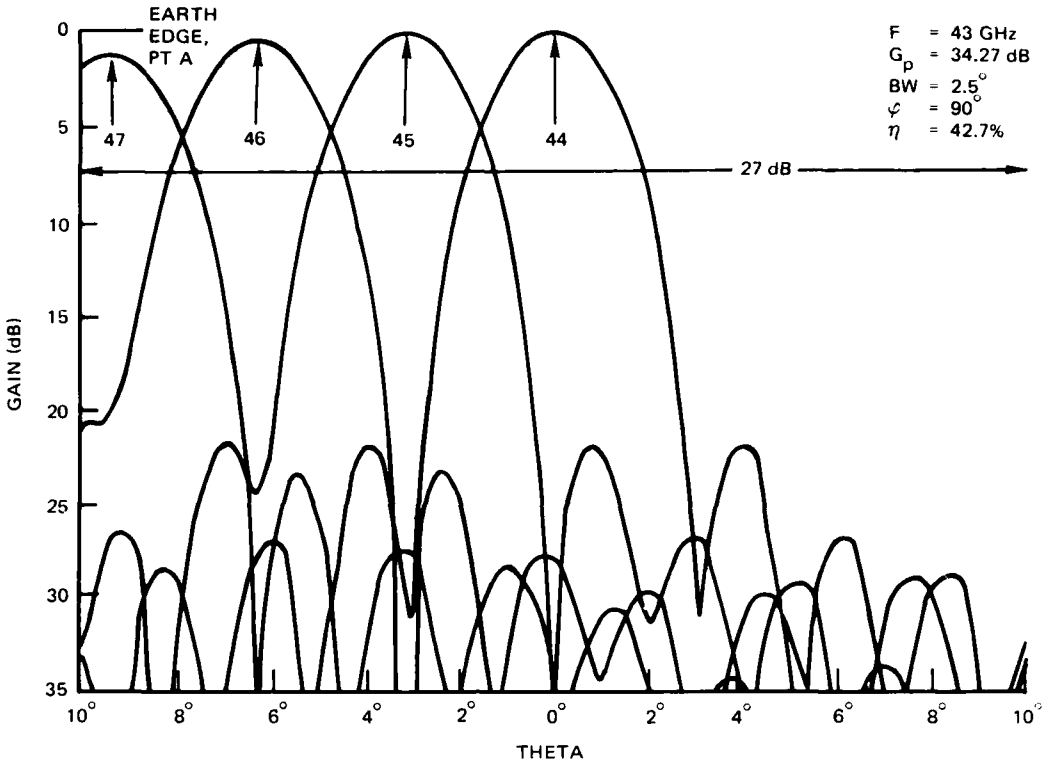

Figure 11a. Predicted lens patterns. (43 GHz, $\phi = 90°$.)

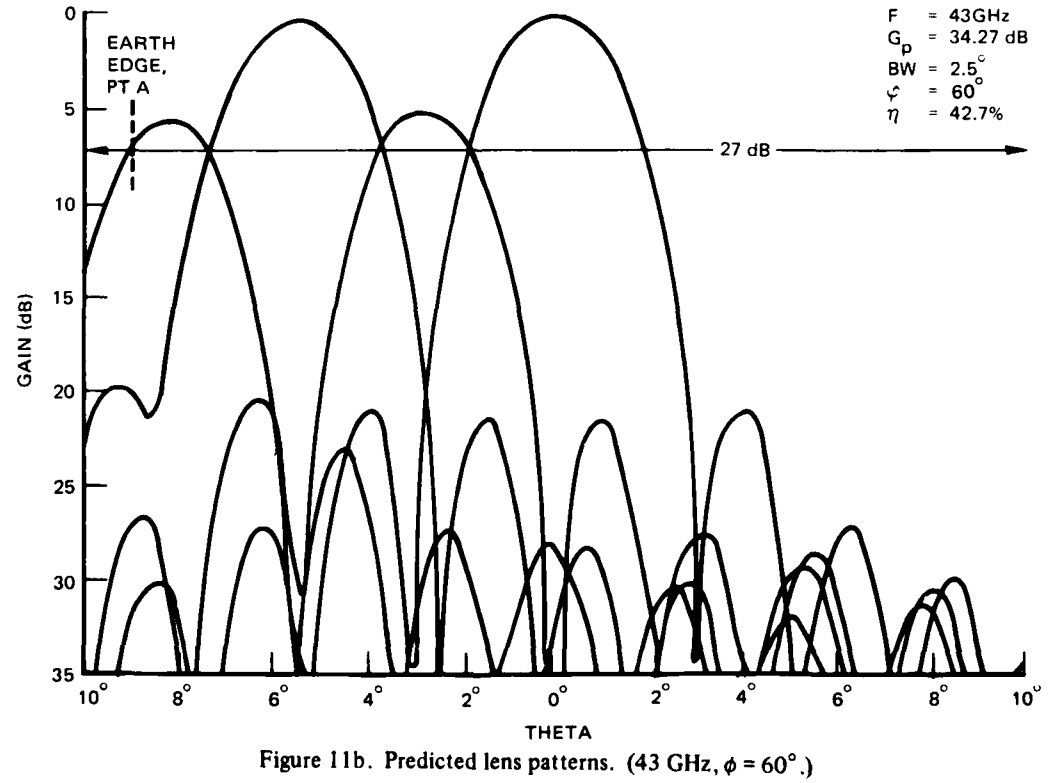

Figure 11b. Predicted lens patterns. (43 GHz, $\phi = 60°$.)

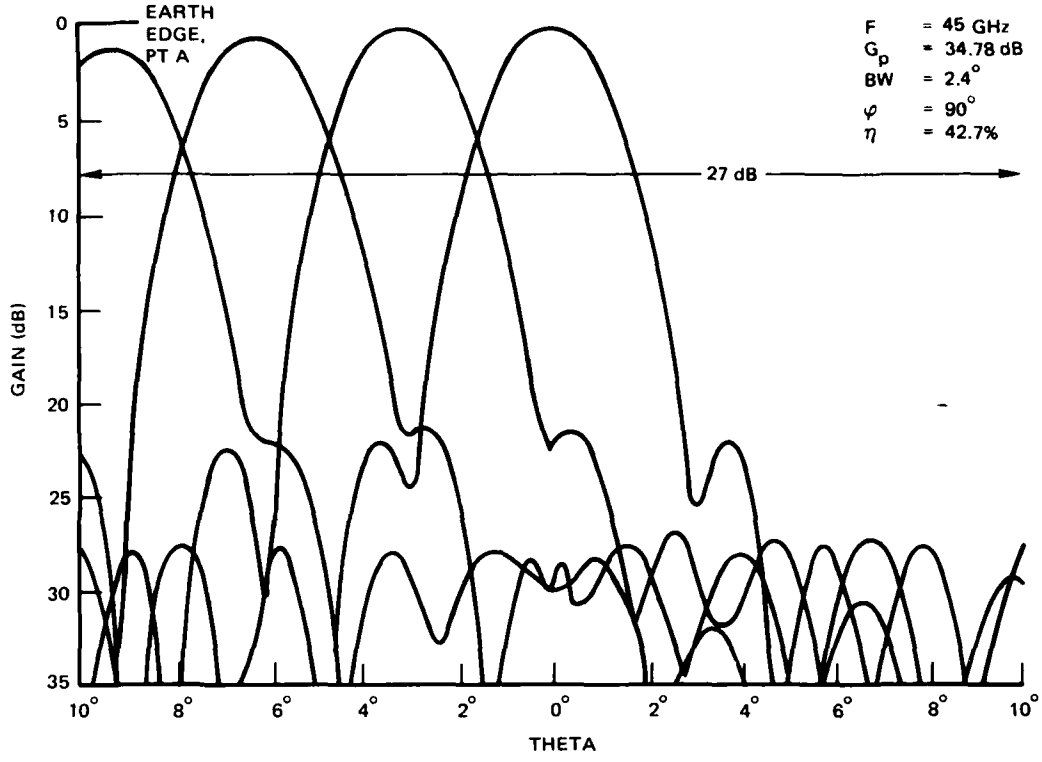

Figure 12a. Predicted lens patterns. (45 GHz, $\phi = 90°$.)

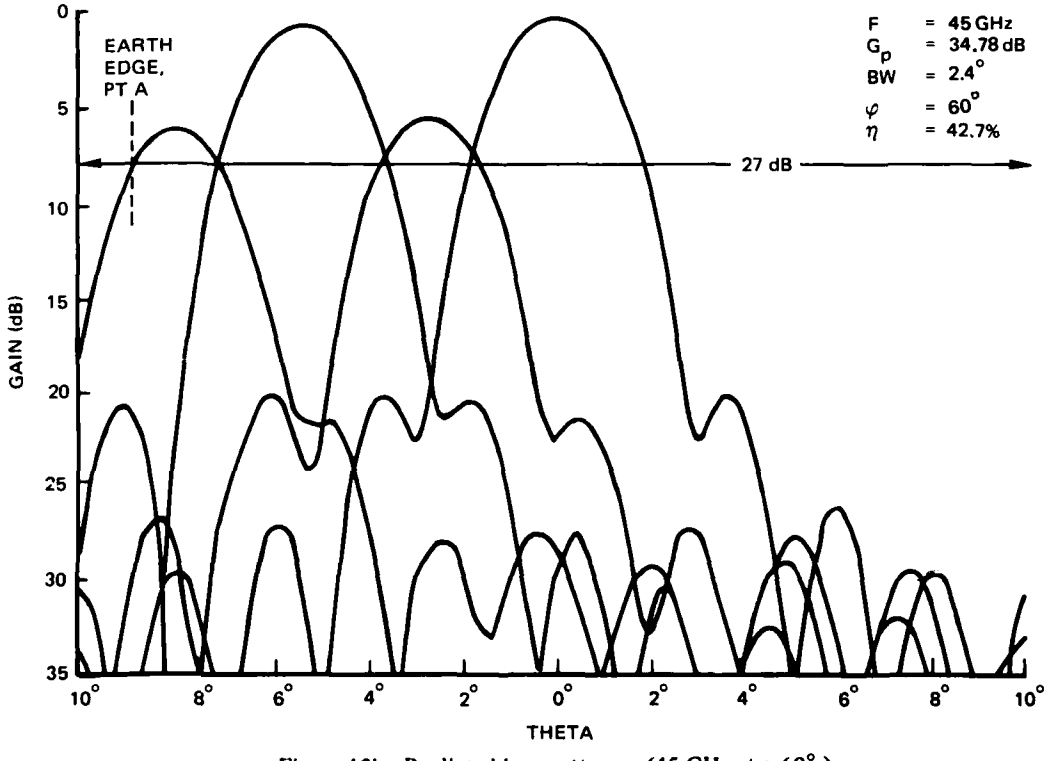

Figure 12b. Predicted lens patterns. (45 GHz, $\phi = 60°$.)

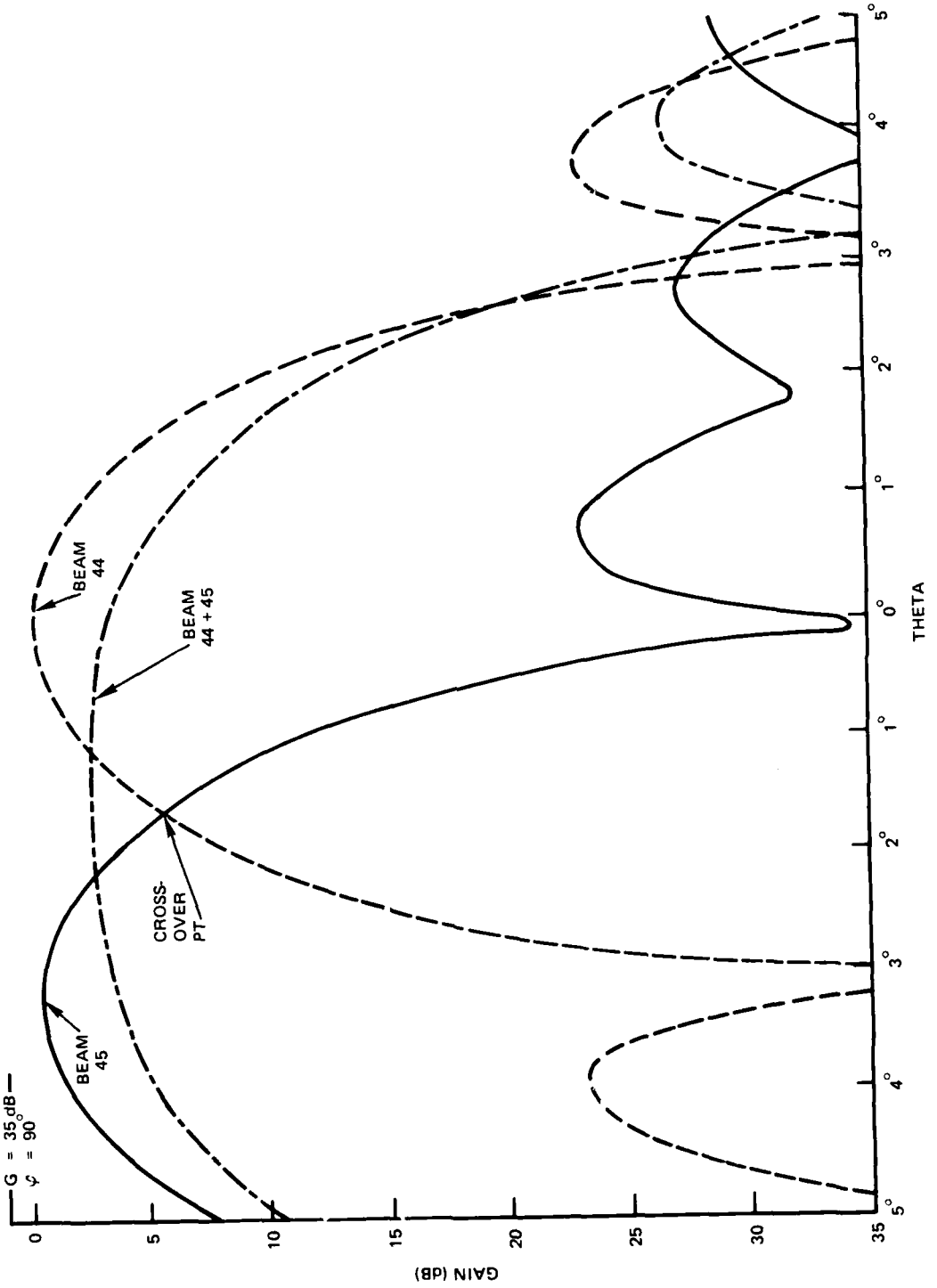

Figure 13. Combining adjacent beams.

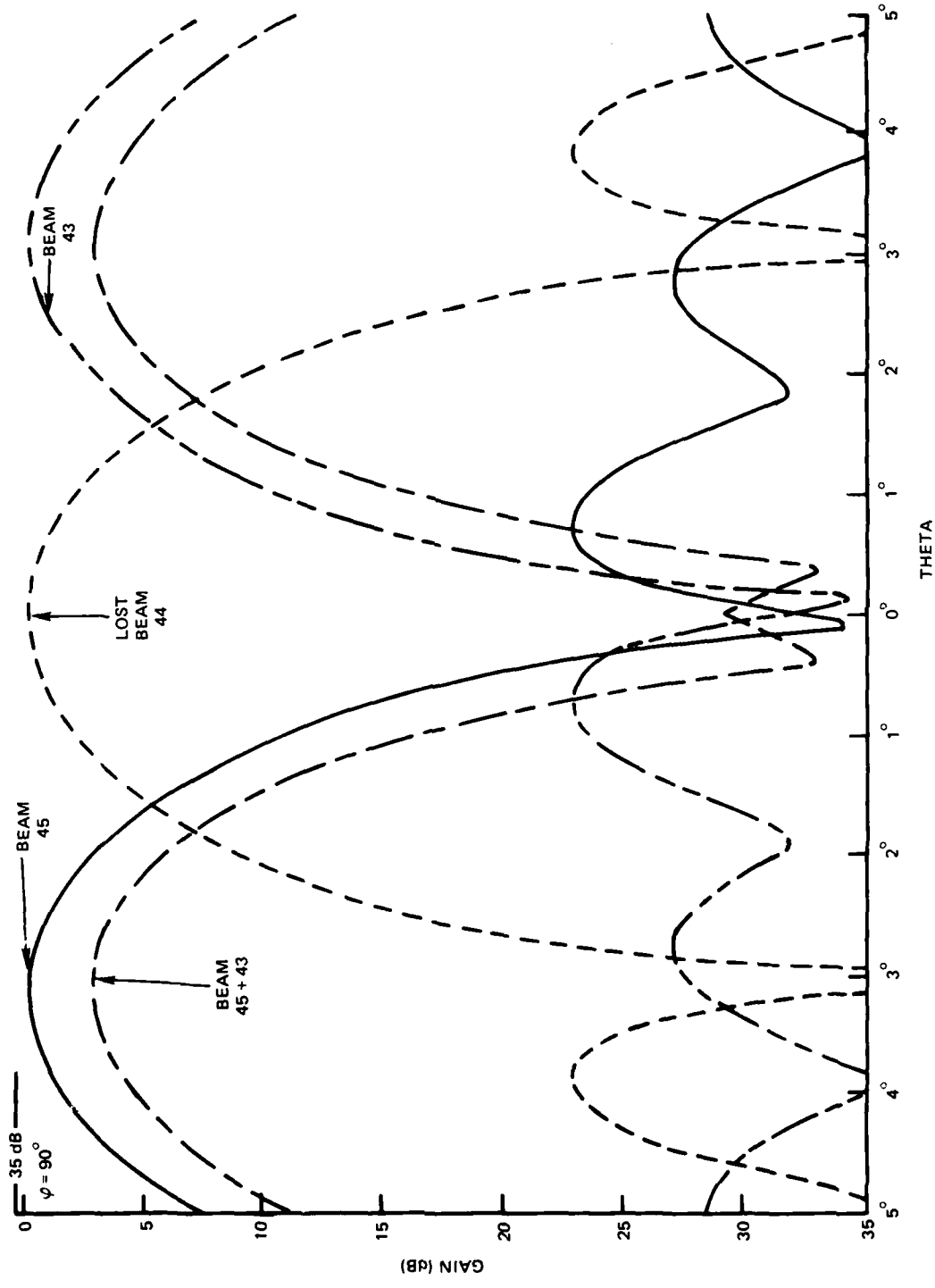

Figure 14. Loss of beam condition (beam 44 lost).

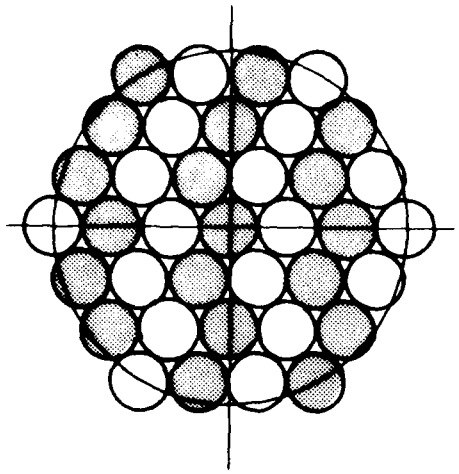

(a) Triangular lattice.

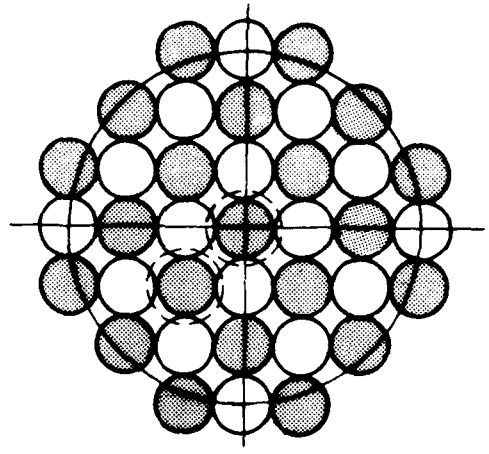

(b) Square lattice (odd).

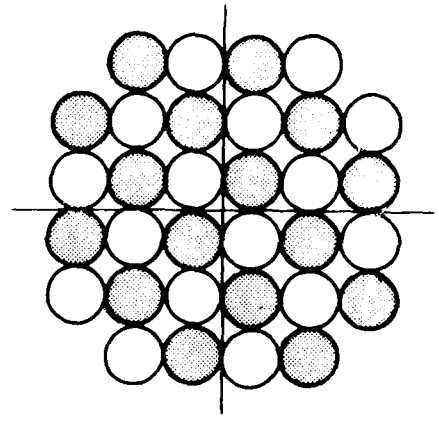

(c) Square lattice (even).

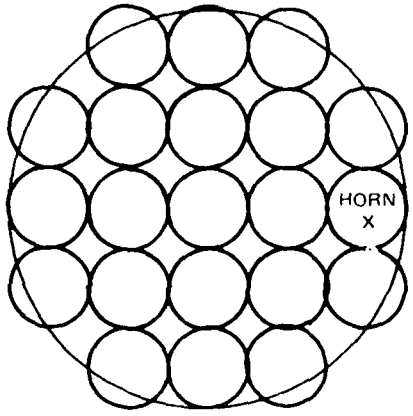

Square lattice odd 21.

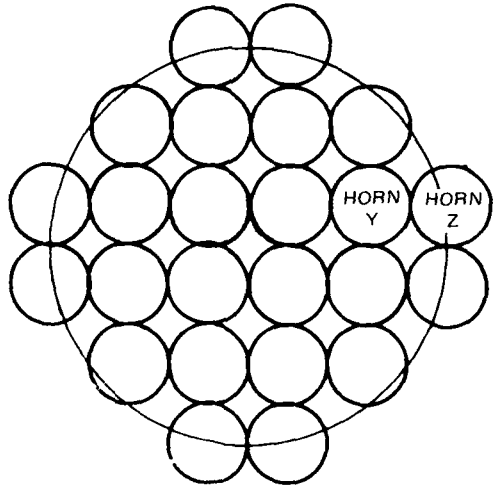

Square lattice even 24.

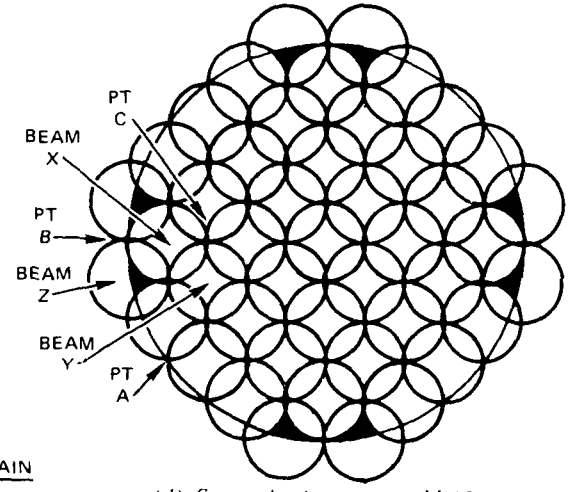

GAIN

PT A: 27.5 dB

PT B: 27.8 dB
27.3 dB

PT C: 28.2 dB
27.9 dB
27.9 dB

(d) Square lattice even + odd 45.

Figure 15. Two-lens consideration.

	Triangular, One-Lens	Even-Square, Two-Lens	Odd-Plus-Even-Square, Two-Lens
D	6.9 inches	5.72 inches	6.16 inches
E1	37	32	45
G_P	34.5 dB	33.2 dB	33.6 dB
G_{MIN}	27 dB	25.7 dB	27.5 dB
BW	2.46°	3.01°	2.77°
η	43.4%	46.1%	44.3%

Table 1. Comparison: one- and two-lens systems.

There is one additional advantage (and disadvantage) to the odd-plus-even-square lattice: its beams overlap at high gain values. As seen from figure 15d, beam X is overlapped by four other beams: beams Z and Y and their mirror images. The advantage is that if beam X is lost, any two, three, or four of the four beams overlapping it can be used to cover the beam X surface area. Figure 16 shows the case where beams Y and Z are summed. Note that the degradation in gain from beam X is $\leqslant 10.2$ dB (without summing Z and Y, the gain would be down ~12 dB). The disadvantage is that if beam X is jammed, the four beams overlapping it will also be jammed, which will result in five beams not being usable.

It was concluded that the advantages of a two-lens system were quite small, and thus the triangular-lattice one-lens system would be used in this design.

4.0 MIXER MATRIX DESIGN

Once the feed horn has received a signal, it is necessary to downconvert the frequency and amplify the signal to establish the noise level and thus the sensitivity of the system. Downconversion occurs by "mixing" the original rf signal with a local oscillator signal (LO) in a non-linear device (ie, a diode). The diode output will consist of LO and rf signals; the higher-order harmonics of LO and rf; the higher-order products of mrf ± nLO (m and n being integers $\geqslant 1$); and a dc output. This output is filtered to yield rf – LO = IF (intermediate frequency), which is applied to an IF amplifier. The noise figure of the system is thus

$$NF_S = L_C + 10 \log_{10}(NF_{IF} + T-1)$$

where L_C is the mixer conversion loss (ratio of rf input power to IF output power), T is the diode noise temperature ratio, and NF_{IF} is the noise figure of the IF amplifier. T is typically 1, giving:

$$NF_S = L_C + NF_{IF} \text{ (in dB)}.$$

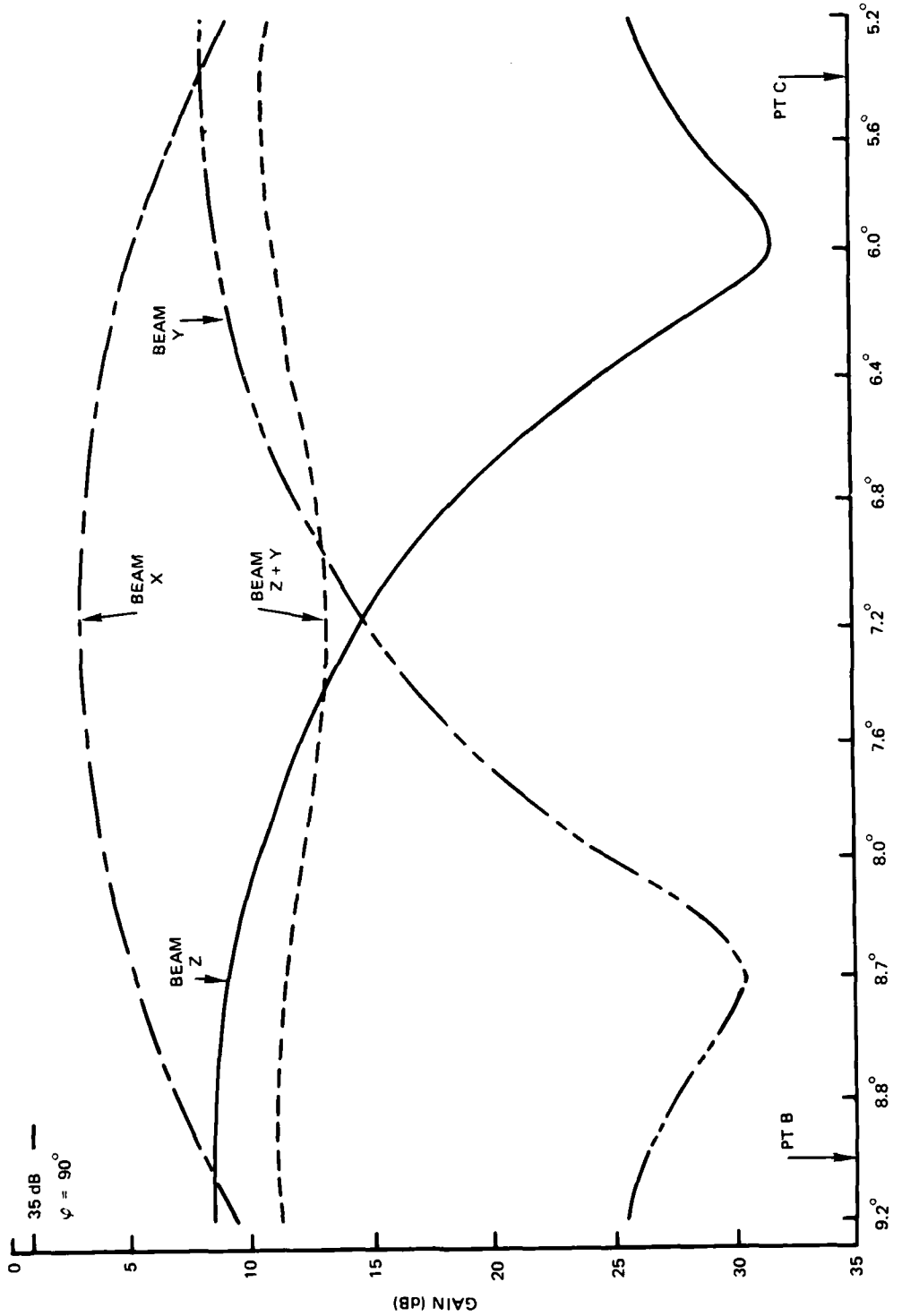

Figure 16. Loss of beam X with odd-plus-even-square lattice.

The conversion loss of a mixer is proportional to $C_j R_s$, and the diode cutoff frequency is given by $F_{CO} = 1/2\pi C_j R_s$ where C_j and R_s are the capacitance and series resistance of the diode.

There are three basic mixer types: the single-ended (unbalanced), the single-balanced, and the double-balanced (ref 5). Each type is depicted in figure 17 and their advantages and disadvantages are compared in table 2. In addition, biasing the diodes will allow for the use of less LO power (ref 6), as shown in figure 18. A biased single-balanced mixer, when compared to a double-balanced mixer, thus may have:

- Lower LO/rf leakage levels
- Equivalent conversion loss
- 10 to 14 dB less LO power required
  (also requires less LO power than single-ended mixer)
- Much lower VSWR
- Much lower cost and less complexity.

The biased single-balanced mixer design was thus chosen. The configuration chosen was a modified rat race (see figure 19), which simplifies construction in microstrip and biasing [ref 7].

The diodes for this mixer design were chosen to minimize the mixer conversion loss; that is, for their small capacitance value. Alpha DMK-6606A diodes (C = 0.06 pF) were selected for the initial units. Diodes with a capacitance of 0.02 pF have also been fabricated by Alpha and could have been made available for this effort. However, they are extremely difficult to work with, susceptible to damage, and several times more expensive.

The decision was made to use an off-the-shelf IF amplifier. Table 3 presents a review of those identified. The WJ-6621-332 was purchased.

As stated in the previous section, a prime concern for this system is the possibility of losing a beam. The probability of a beam loss depends on the mean-time-to-failure (MTTF) of its components. Each beam has associated with it the lens, a horn, a mixer, and an IF amplifier. The lens and the horn are passive devices and can be neglected. The MTTF values for the IF amps and the diodes in the mixer are as follows:

IF amp: > 125 000 hours standard
> 2 500 000 hours high-reliability type
Diodes (6606 or 4791): > 175 000 hours

---

5. Reynolds, J.F., and M.R. Rosenzweig, Learn the Language of Mixer Specifications, Microwaves, p 74 and 76, May 1978.
6. Anaren Catalog, p 159.
7. NOSC TN 550, MIC Millimeter-Wave Channelized Downconverter, by D. Rubin and D Saul, p 13 and 15, 11 October 1978.

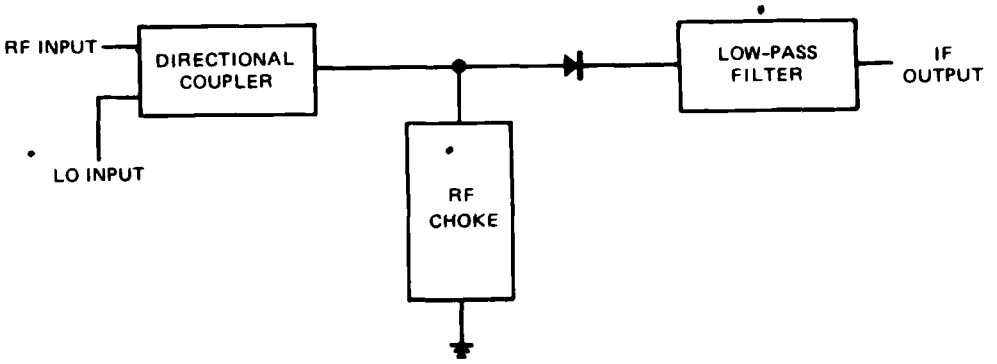

Figure 17a. Single-ended mixers.

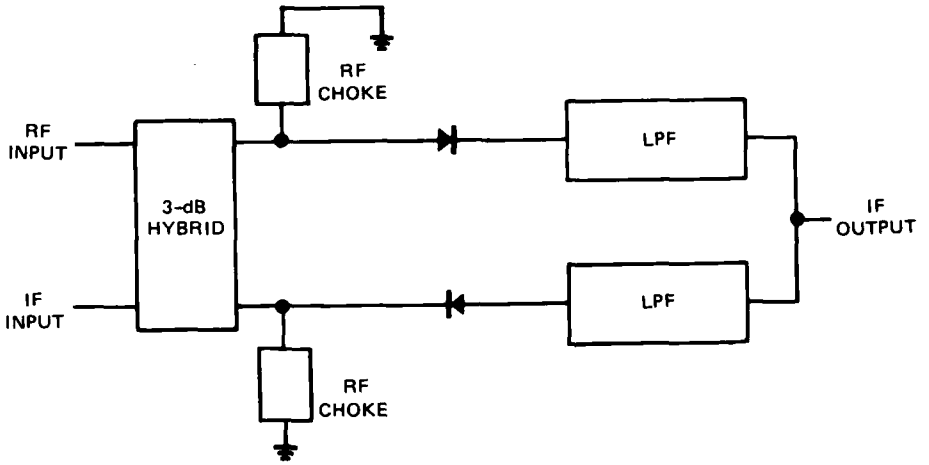

Figure 17b. Single-balanced mixers.

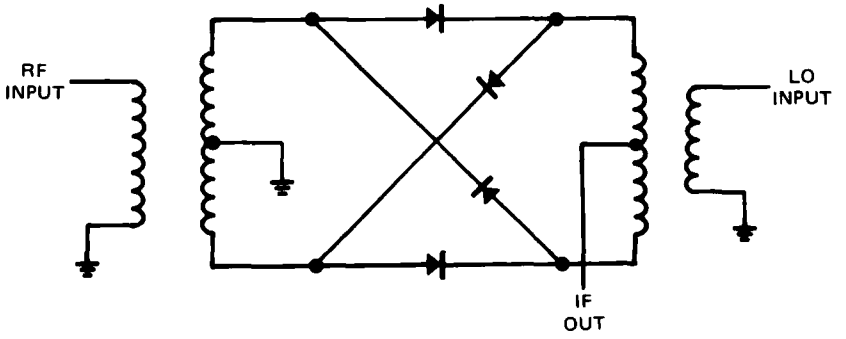

Figure 17c. Double-balanced mixers.

Single-Ended	Single-Balanced	Double-Balanced
Advantages: • One diode • Simplicity • Less LO power needed Disadvantages: • No LO AM noise suppression • rf/LO coupling mechanism necessitates higher LO power than required by diode • Little/no LO radiation protection • Smallest dynamic range • Poorest IM performance • Poor VSWR	Advantages: • AM noise cancellation • Reduced LO radiation • Efficient use of LO power • Easily constructed in microstrip • Easily biased • Good VSWR • Improved IM performance • Improved dynamic range Disadvantages: • Two diodes required • More LO power required	Advantages: • Lowest conversion loss • Best IM performance • Best isolation • AM noise-cancellation • Improved dynamic range Disadvantages: • Four diodes required • Requires most LO power • Poor VSWR • Complexity • Difficult to construct or bias

Table 2. Basic mixer types.

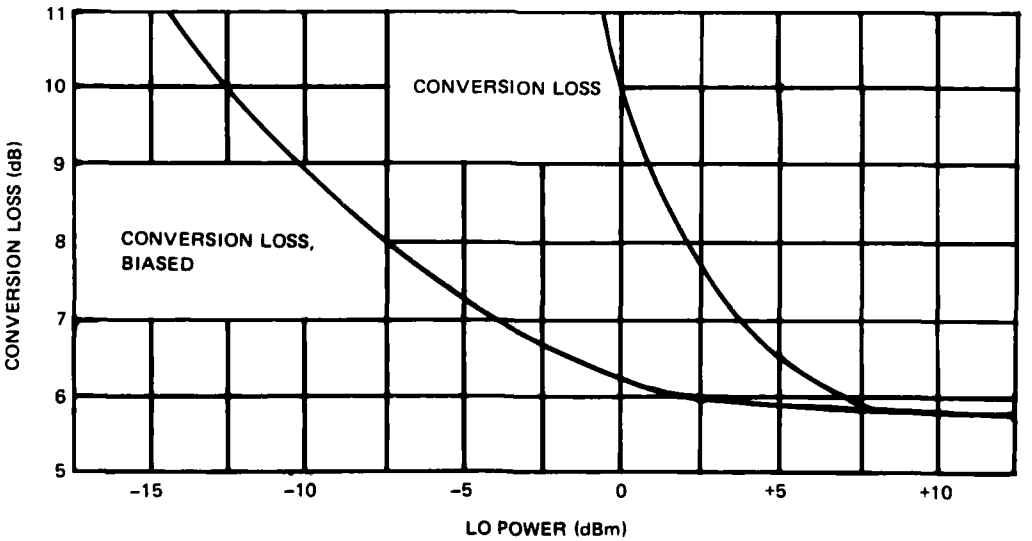

Figure 18. Comparison of biased versus unbiased diode performance with LO power.

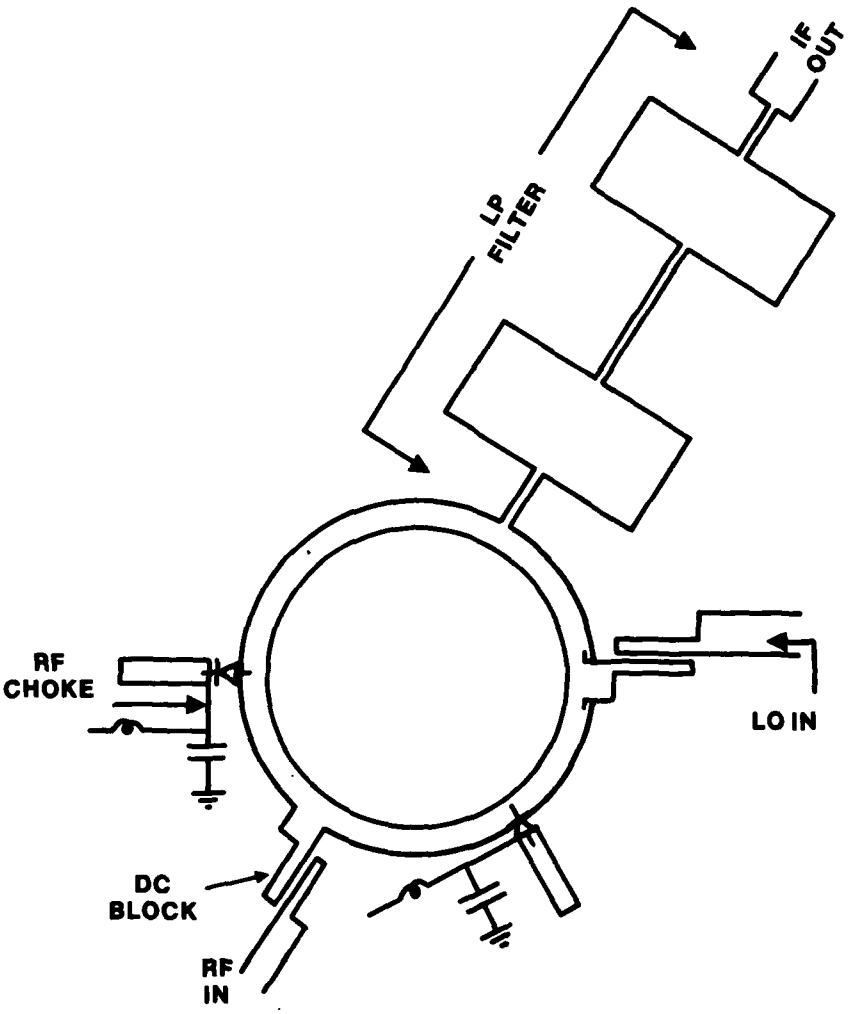

Figure 19a. Modified rat-race mixer.

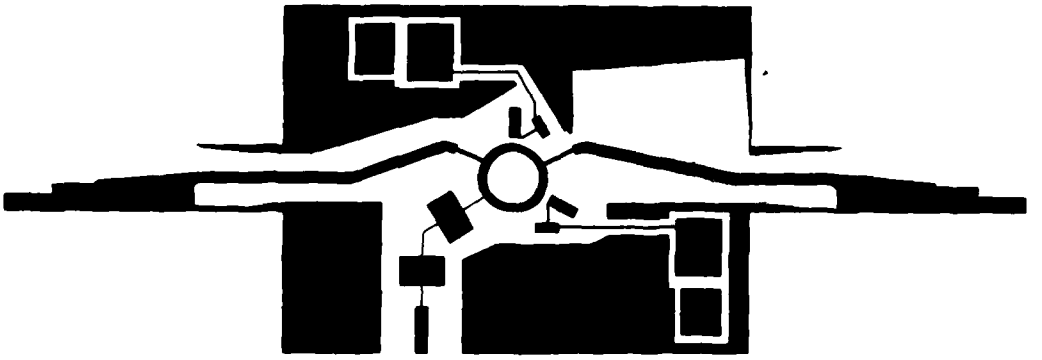

Figure 19b. Enlarged transparency of modified rat-race mixer.

Source	Model	NF, dB	Gain, dB	Price, $
NARDA	N6233S-9	3	40	2200
AVANTEK	AMG-4032	4.5	42	920
AMPLICA	301-SSL	4.5	29	1550
Watkins/Johnson	WJ-6621-332	3.0	30	1560
TROU-TECH	In development – not yet available	2.5	–	–

Table 3. 2-4-GHz IF amplifier review.

Assuming that the failure of one diode equates to loss of the beam, the probability that a beam will not be lost in t hours is

$$P = e^{-(\lambda_{IF} + 2\lambda_D)t}$$

where $\lambda = 1/MTTF$. If a diode failure appears in the design presented, this will be true. Assuming that the diodes can be made to operate independently, the probability that a beam will not be lost is

$$P_B = e^{-\lambda_{IF}}\left(2\,e^{-\lambda_D t} - e^{-2\lambda_D t}\right)$$

and the probability of degraded performance not occurring is

$$P_{DEG} = e^{-(\lambda_{IF} + 2\lambda_D)t}.$$

The system requirement is, however, that every beam work simultaneously. The probability of any of the 37 beams failing must be considered. Since all beams are identical, the probability of none of the 37 beams failing is

$$P_s = (P_B)^{37}.$$

The system reliability design goal is $P_s \geq 0.9$ for at least 5 years. Table 4 presents the probability values of P_s over various lengths of time and with various levels of redundancy. Note that with no redundancy and one diode failure resulting in beam loss, the probability of surviving for 1 year is only 2.16%. Assuming fourfold redundancy (148 mixers and 148 IF amps) and that one diode loss results in degraded performance, the probability of surviving for 5 years is 99.93% and the probability of not degrading is 36.6%. [If single-ended mixers had been used in the design, the probability of surviving for 5 years (with fourfold redundancy) would be 89.29% but, of course, the probability of not degrading would be 100% since there would be only one diode per mixer.] The price of having simultaneous beams is thus seen to be the need for a high level of redundancy and/or soft fail mixers.

1 diode loss = failure or $P_S = P_{DEG}$.

No Redundancy

P_B	t, yr	P_S
0.9015	1	0.0216
0.8127	2	0.0005
0.7327	3	0
0.6605	4	0
0.5954	5	0

Twofold Redundancy

P_B	t, yr	P_S
0.9903	1	0.6972
0.9649	2	0.2668
0.9286	3	0.0644
0.8847	4	0.0108
0.8363	5	0.0013

Threefold Redundancy

P_B	t, yr	P_S
0.9990	1	0.9652
0.9934	2	0.7836
0.9809	3	0.4899
0.9609	4	0.2283
0.9338	5	0.0792

Fourfold Redundancy

P_B	t, yr	P_S
0.9999	1	0.9965
0.9988	2	0.9554
0.9949	3	0.8277
0.9867	4	0.6095
0.9732	5	0.3660

2 diode loss = failure.

No Redundancy

P_B	t, yr	P_S
0.9941	1	0.8034
0.9840	2	0.5503
0.9703	3	0.3274
0.9536	4	0.1722
0.9344	5	0.0812

Twofold Redundancy

P_B	t, yr	P_S
1	1	0.9987
0.9997	2	0.9906
0.9991	3	0.9679
0.9978	4	0.9234
0.9957	5	0.8525

Threefold Redundancy

P_B	t, yr	P_S
1	1	1
1	2	0.9999
1	3	0.999
0.9999	4	0.9963
0.9992	5	0.9896

Fourfold Redundancy

P_B	t, yr	P_S
1	1	1
1	2	1
1	3	1
1	4	0.9998
1	5	0.9993

Table 4. Probability of 37 beams surviving t years.

The physical layout of the mixer matrix presents a considerable problem since each horn in figure 5b must have its own mixer, IF amp, and LO power supply. A tentative design for the mixer matrix is shown in figure 20. The mixers will be formed on seven printed circuit boards. Each board will hold five to seven mixers and be attached to a corresponding number of horns and IF amps (figure 20a). The LO power will be distributed to each board by means of waveguide broadwall couplers [ref 8], as shown in figure 20b. The LO power is distributed within the boards by using microstrip N-way power dividers [ref 9], as shown in figure 20c. The overall LO power distribution is depicted in figure 21.

5.0 DEMONSTRATION SYSTEM FABRICATION AND TEST

To demonstrate the capabilities of this design, the lens, the feed horns (six with polarizers mounted in them), a mixer, and an IF amplifier were fabricated or procured. These components, and their test results, are discussed in the following paragraphs.

5.1 MIXER AND IF AMPLIFIER

Two mixer configurations were derived, both based on the rat-race design depicted in figure 19. The first was constructed on 5-mil Duroid microstrip. Its conversion loss was 8 to 9 dB across the 43-to-45-GHz bandwidth on an LO power level of 2 milliwatts. The problem with this design, as indicated in section 4, is that if one diode fails, the whole mixer fails. Thus a second mixer design was attempted which would isolate the diodes to some degree. This would create a soft fail mixer in which the conversion loss would deteriorate by no more than 6 dB if one diode failed and P_S = 85.25% with twofold redundancy (see table 4).

The new mixer design is shown in figure 22. The basic change is that the IF signals are taken from behind each diode and combined in a Wilkinson-type power combiner [ref 9] with an isolation resistor. This circuit was cut in 10-mil Duroid microstrip.

The results of tests on the second design are presented in table 5. The conversion loss was 8.8 to 9.6 dB for an LO power of 2 milliwatts; ie, about one-half dB higher than on the first design. With 5-milliwatt LO power, however, the conversion loss is reduced to a range of 8.2 to 9.0 dB across the band. The desired VSWR was 2.0:1 or less, which was achieved at rf but missed slightly (2.1:1) at IF. This second design was of the soft failure type. The degradation in conversion loss with one diode failed varied from 3.0 to 6.2 dB. The average degradation was 4.5 dB from 43 to 44 GHz and 5.5 dB from 44 to 45 GHz; thus 5 dB was taken to be the typical degradation value.

An FET low-noise amplifier was purchased from Watkins/Johnson (WJ-6621-332) and specified for a 3-dB noise figure, 30-dB gain over the 2-to-4-GHz IF bandwidth. The unit showed a gain of 33.8 to 35.4 dB and a noise figure of 1.8 to 2.3 dB, with a VSWR of less than 2.0:1.

---

8. Levy, R., Directional Couplers, Advances in Microwaves, v 1, 1966.

9. Saleh, A.A.M., Planar Electrically Symmetric N-Way Hybrid Power Dividers/Combiners, IEEE T-MTT-28, p 555-563, June 1980.

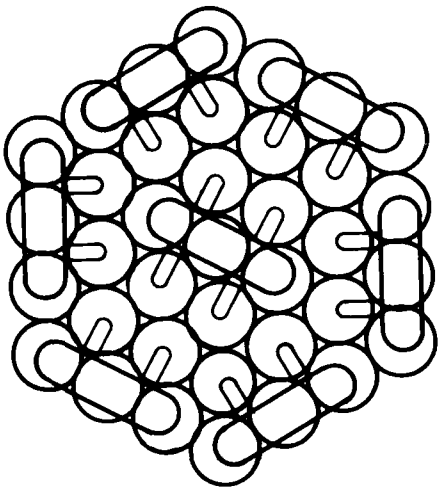

(a) Mixer matrix, 7 boards, 6-5 mixers, 1-7 mixers.

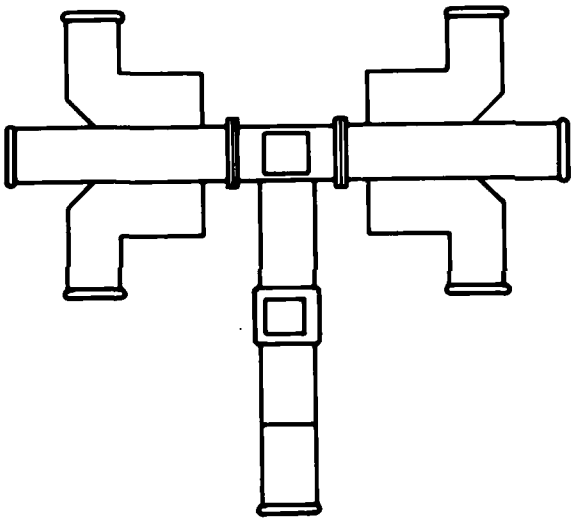

(b) LO power split to boards, 7-way.

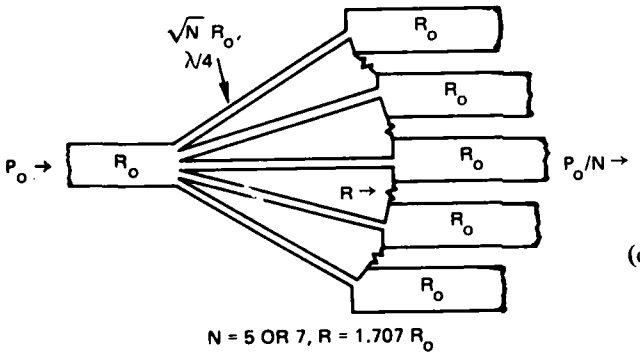

(c) N-way power divider for mixer board.

Figure 20. Mixer matrix design.

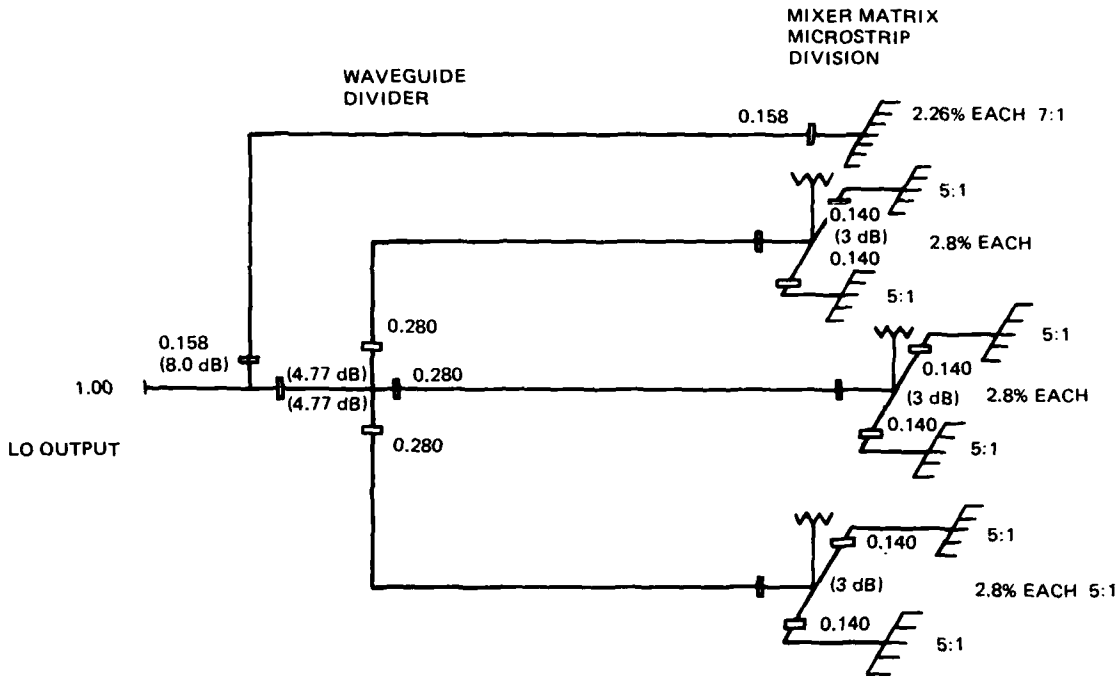

Figure 21. LO power distribution.

5.2 FEED HORNS AND POLARIZERS

The feed element design was a simple conical horn, as shown in figure 23. The horns were fabricated in the Public Works shops at NOSC. Element antenna patterns are shown in figure 24. The gain across the frequency band was 15.35 to 15.85 dB. Gain and efficiency (~79%) were better than predicted. A dielectric-loaded horn was purchased from TRG* for comparison purposes. The TRG horn had gains of 16.2 to 16.7 dB across the band (~91% efficiency).

The feed horns were mounted in a feed fixture of the design shown in figure 25 (see also figure 26). It was found that when the horns were placed in the feed structure in such a way that they extended beyond it by one-quarter wavelength, the gain of the conical horns increased by about 1 dB. (The six adjacent elements were loaded during gain measurements.) This arrangement was used on all other tests.

The isolation between the horns was also measured. The desire was to have at least 30 dB of isolation. (Isolation here is the amount of attenuation of signal from one horn which is coupled to another horn.) Figure 27 shows the measured values of isolation. Note that it is more than 45 dB except at one point (at 43 GHz in the H-plane, it is about 43 dB).

Figure 28 shows the measured VSWR of a feed horn. The VSWR tends to be less than 1.1:1, even when a polarizer is placed into the horn. The polarizer is of the vane type and is made of Noryl (see figure 29). The initial goal was to obtain an axial ratio of better than 2 dB. Three cuts (ie, polarizer dimensions) were tried. After the second cut, the goal

*TRG division of Alpha Industries.

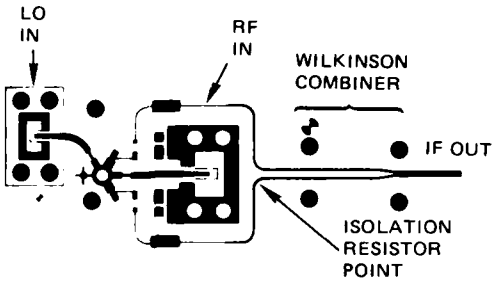

Figure 22a. Soft failure mixer layout.

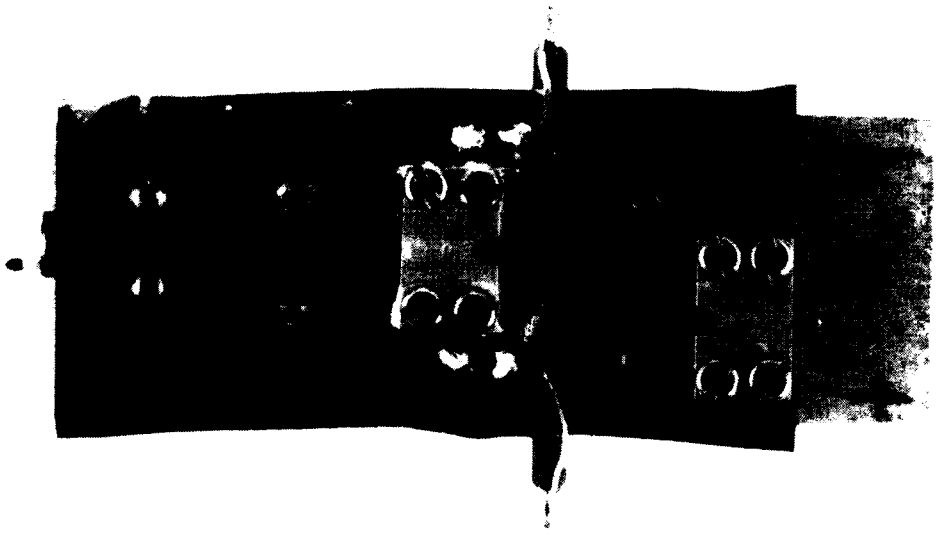

Figure 22b. Soft failure mixer.

rf Freq, GHz	rf Return Loss, dB	IF Freq, GHz	IF Return Loss, dB	Conversion Loss, dB LO Power:			Degradation, One Diode Fail, dB
				2 mW	5 mW	8 mW	
43	16.4	2	9	9.6	9.0	8.4	4.2
43.4	16.6	2.4	9.8	8.8	8.3	7.6	4.5
43.8	19.2	2.8	10.0	9.3	8.7	8.2	4.8
44.2	19.3	3.2	9.0	8.8	8.2	7.5	6.2
44.6	20.0	3.6	9.5	9.4	8.7	8.2	5.5
45.0	15.0	4.0	14.5	9.0	8.3	7.7	4.8
43-45	VSWR $<1.5:1$	2-4	VSWR $\leq 2.1:1$	8.8-9.6	8.2-9.0	7.5-8.4	Typically 5 dB
BIAS = 5 Vdc							

Table 5. Soft failure mixer test.

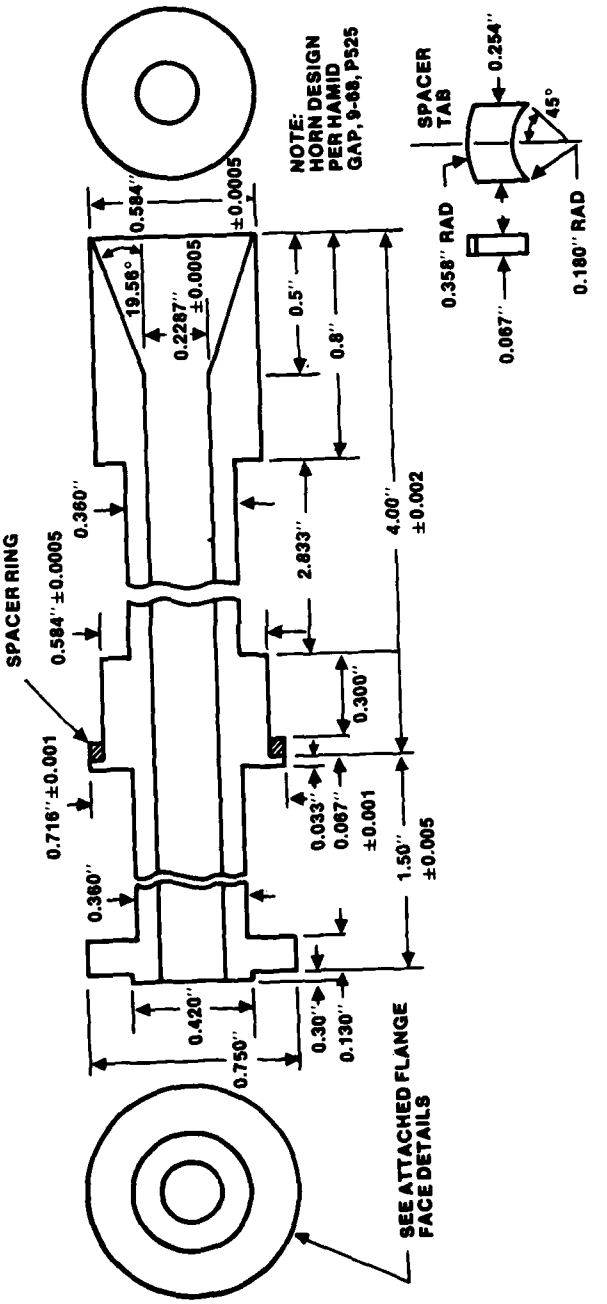

Figure 23. Lens antenna feed horn.

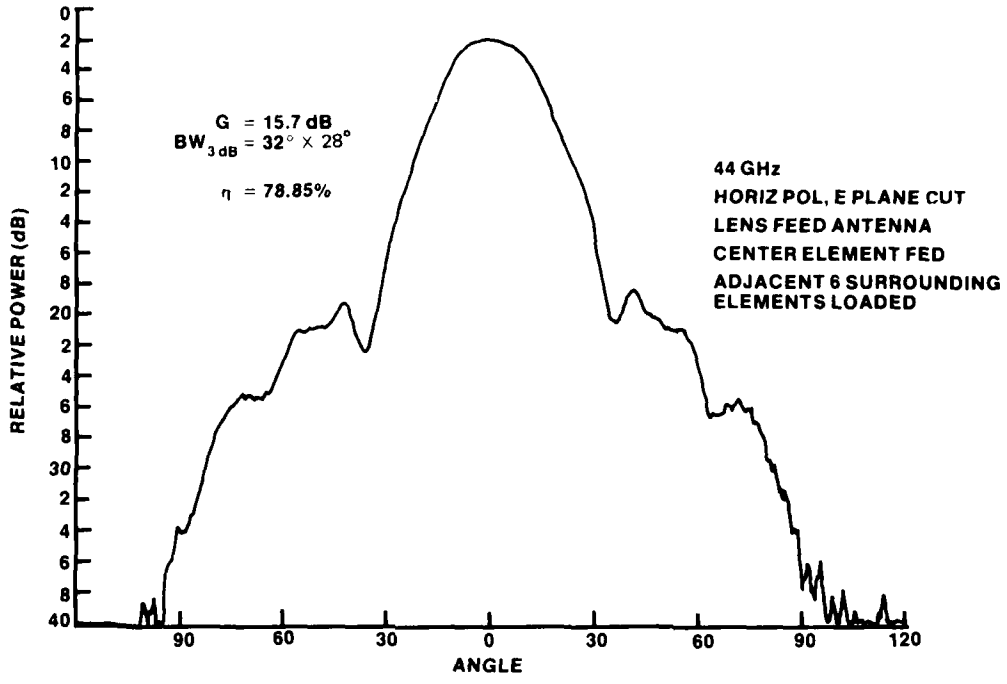

Figure 24a. Horn element antenna pattern.

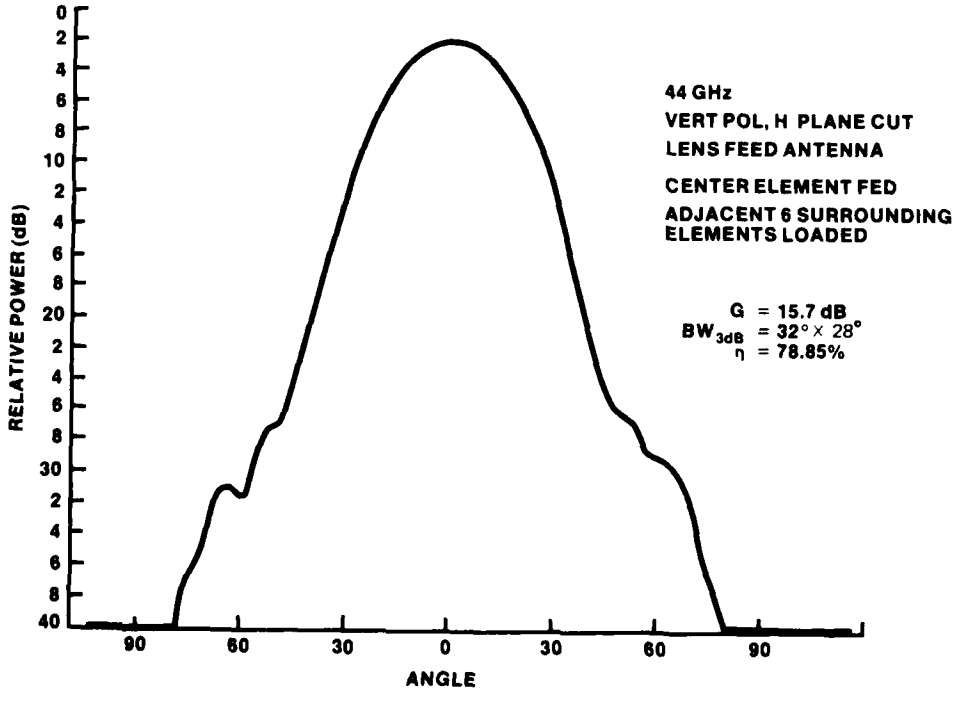

Figure 24b. Horn element antenna pattern.

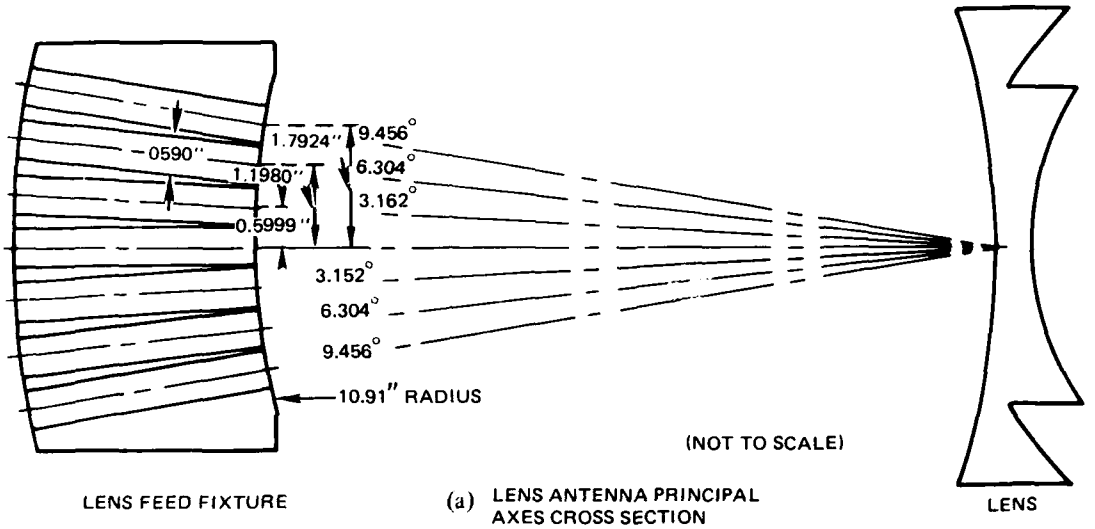

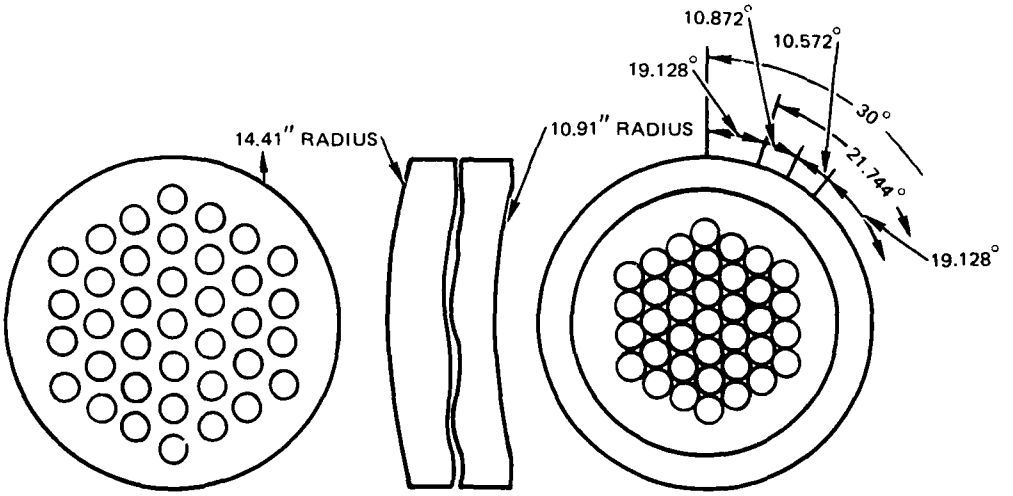

(b) LENS ANTENNA FEED FIXTURE

Figure 25a-b. Lens feed fixture.

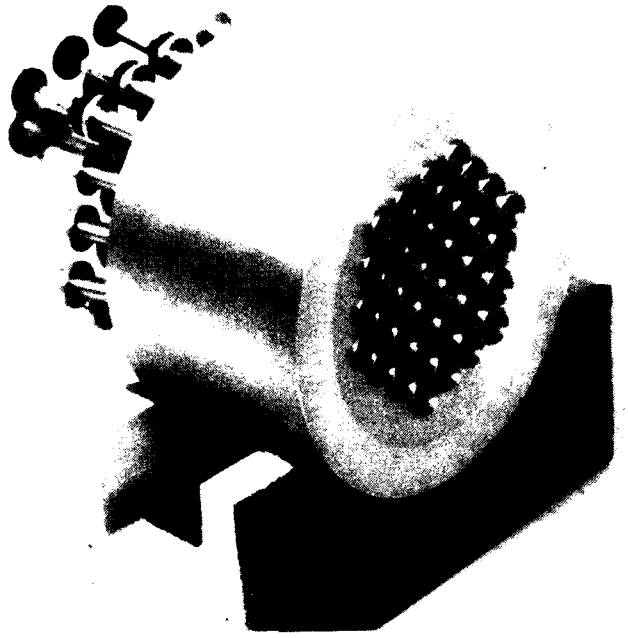

Figure 26a. Feed horns and fixture, front.

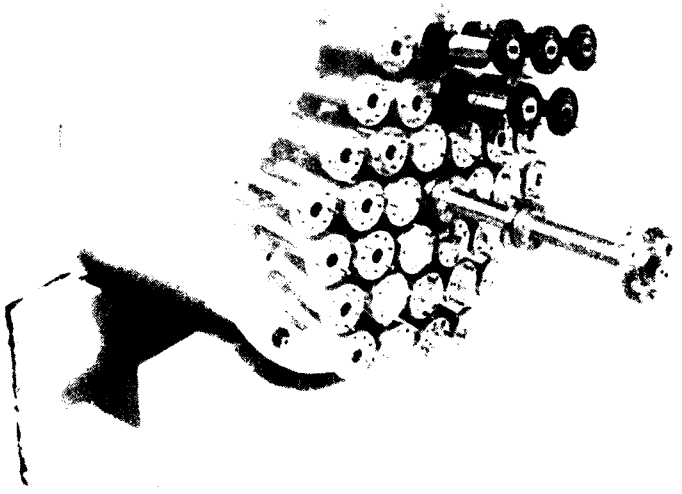

Figure 26b. Feed horns and fixture, rear.

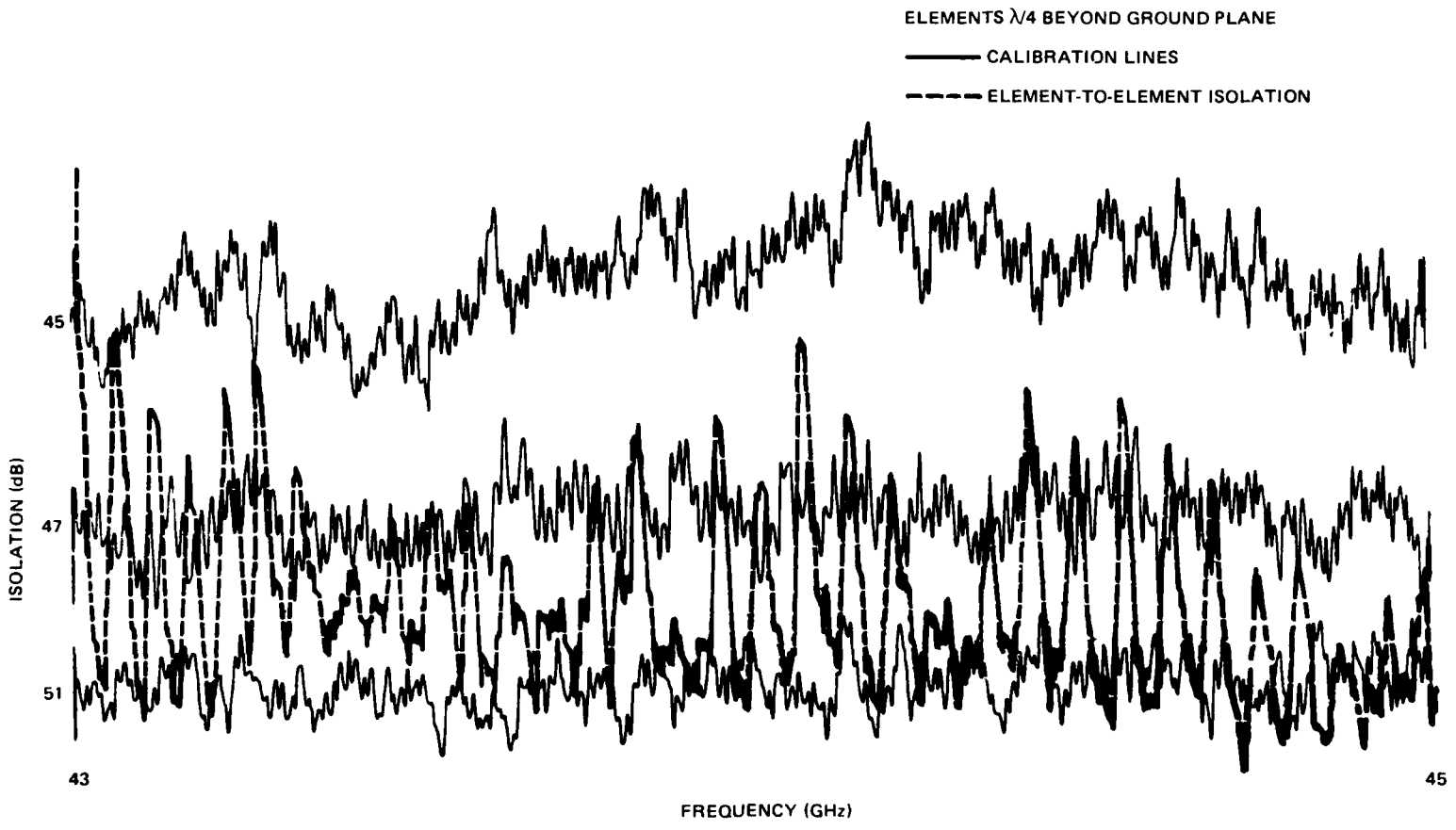

Figure 27a. Lens antenna feed horn H-plane isolation.

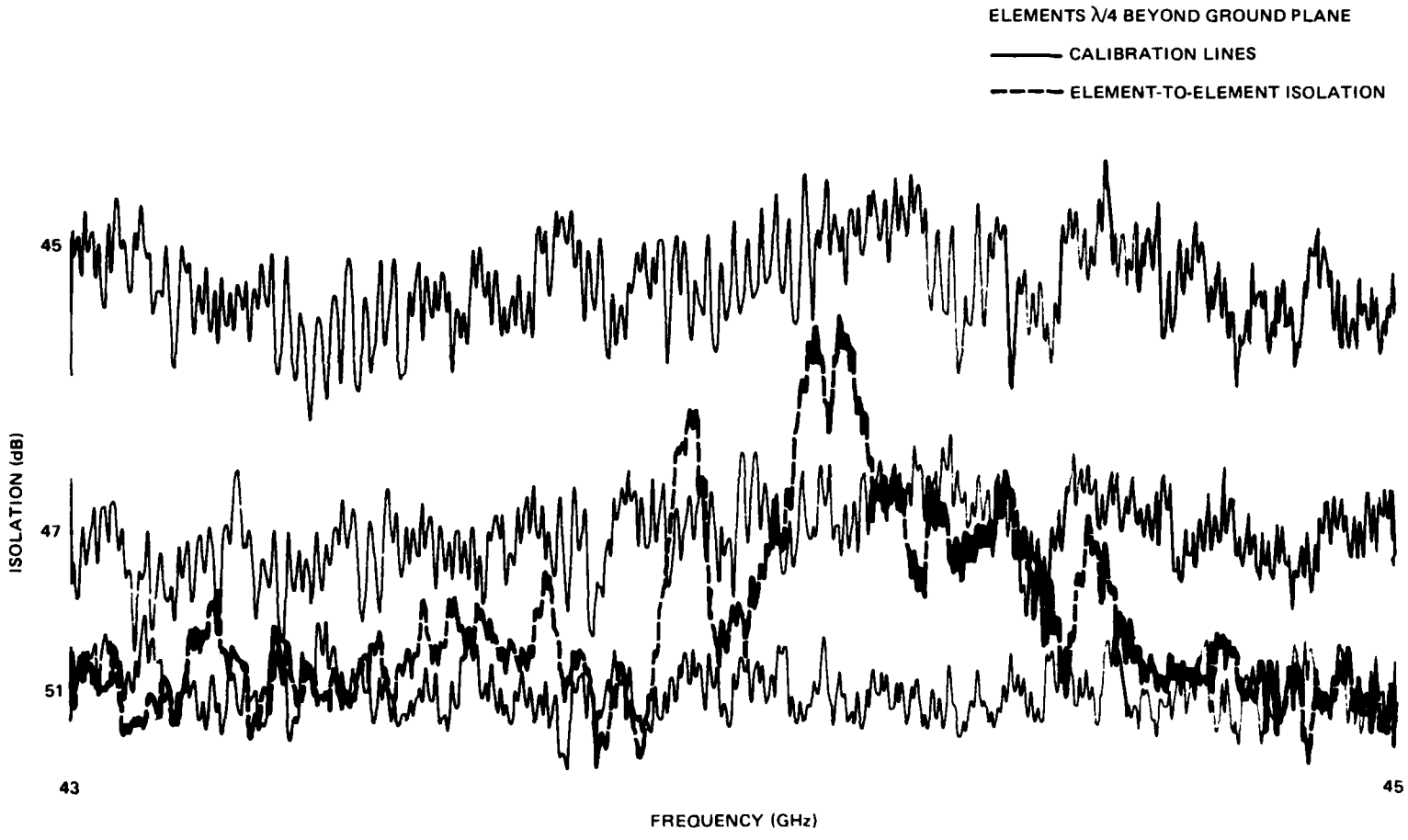

Figure 27b. Lens antenna feed horn E-plane isolation.

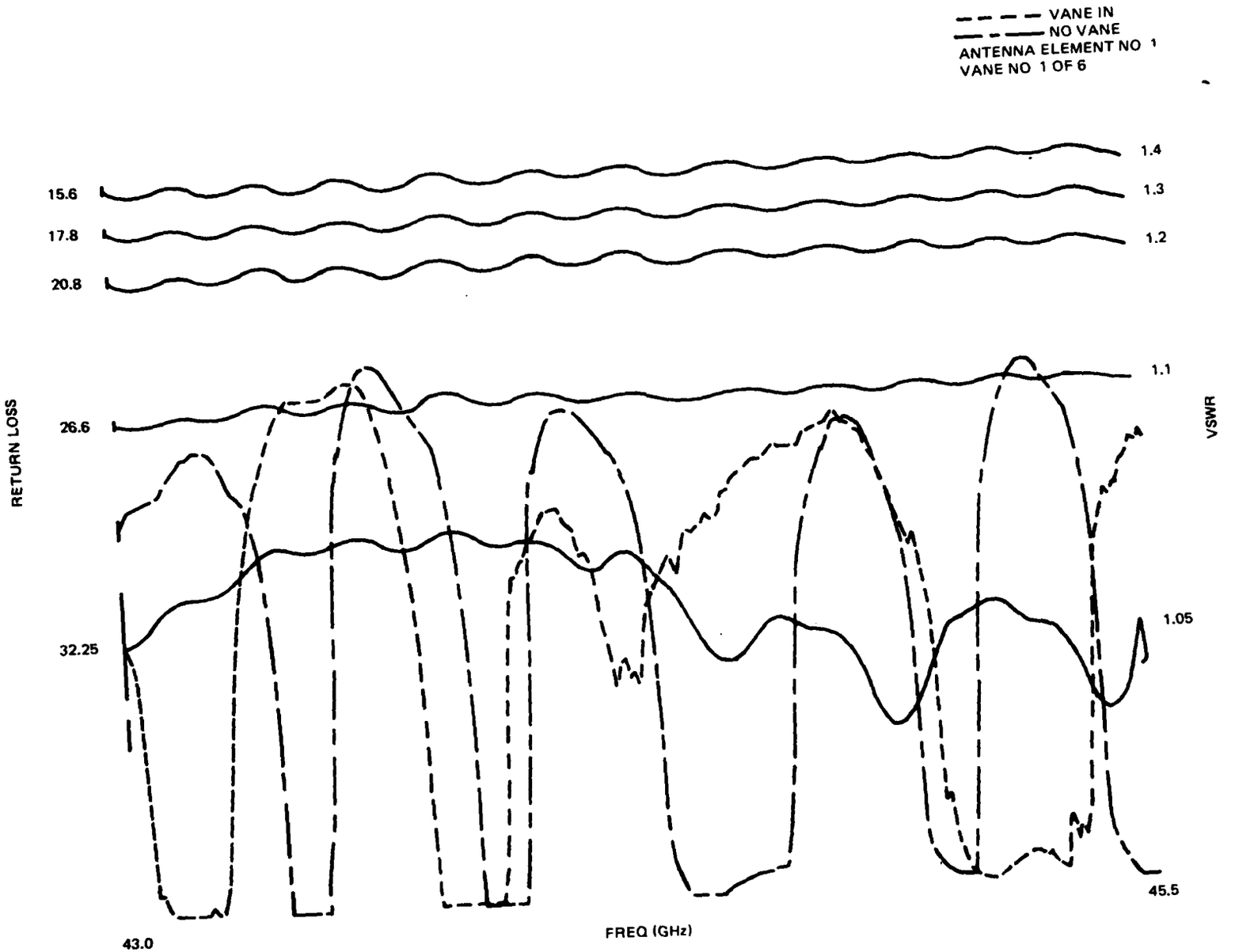

Figure 28. VSWR of horn with and without polarizer.

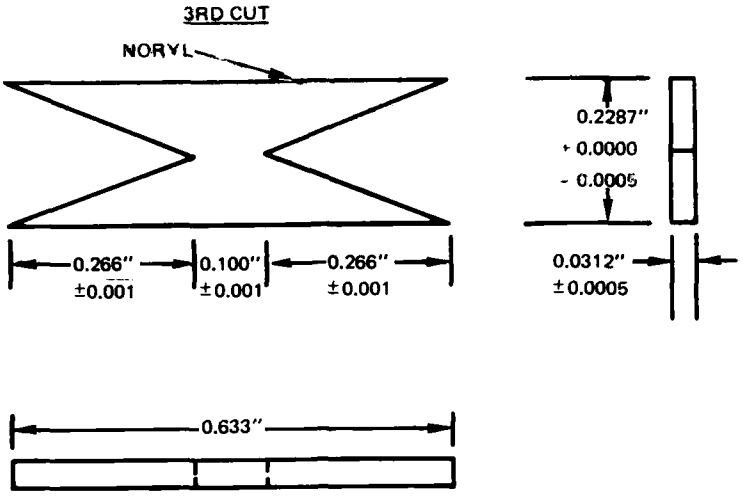

Figure 29. Quarter-wave plate vane polarizer.

became the achievement of six polarizer/horn combinations with an axial ratio of better than 1 dB. Table 6 shows the results. Note that four of the six have axial ratios of 1 dB or less, and that the maximum axial ratio is 1.3 dB.

5.3 WAVEGUIDE LENS

The waveguide lens was fabricated by Gamma-F Corp, in Torrance CA. The lens weighed 2.6 pounds and was 20 mils longer than specified. This increase in length resulted in a constant phase shift and thus no change in lens performance. Of the 716 waveguide sections, seven were measurably off in length. The typical error was 15 mils, the maximum 35 mils. These are well within the specified tolerance of 72 mils. The photo in figure 30 shows the lens as it was mounted for testing.

From a review of the beam patterns desired from the lens (see figure 5a), it is seen that the beam arrangements are repeated every 60° and are symmetrical about the center of any 60° sector. Thus there are only six unique beam positions. The lens performance can thus be depicted by looking at six beams, say beams 44, 45, 46, 47, 55, and 56. An azimuth cut of 90° will pass through the beam peaks of the first four beams listed and also show the maximum crossover points. A cut of 70.9° will pass through the peak of beam 56. A cut of 60° will pass through the peak of beam 55 and also show the minimum gain point. Figures 31a, 31b, and 31c show the patterns measured for these azimuth cuts at the design frequency of 44 GHz. Figures 32 and 33 show the 90° and 60° cuts for the frequencies of 45 GHz and 43 GHz. The results are tabulated in table 7.

From figures 31 through 33, it can be seen that all of the beams are within 0.1° of where they should be except beam 56, which is shifted about 0.2° out. The primary effect of this can be seen in figure 31c, where the gain at the crossover of beams 55 and 56 (27.4 dB) is less than the gain at 9° (28.3 dB). The design was for these values to be equal.

The slight misalignment of beam 56 may have reduced the minimum gain by a few tenths of a dB, but even so it exceeds the 27-dB specified level. Efficiency ranged from 41.6% to 43.5%. The sidelobes were more than 21 dB down at 44 GHz and 45 GHz, but at 43 GHz rose to 19.8 dB down.

Freq, GHz	AXIAL RATIO, dB					
		Polarizer Number:				
	2 of 6	3 of 6	4 of 6	5 of 6	6 of 6	II
43	0.3	0.1	0.5	1.2	0.6	0.7
43.5	0.6	0.8	0.1	0.75	0.2	0.25
44.0	0.1	0	0.3	0.9	0	0.4
44.5	1.3	0.75	0.6	0.3	0.5	0.2
45.0	0.7	0.4	0.1	0.6	0.3	0.75

Table 6. Axial ratio measurements.

The dielectric-loaded horn was also tested with the lens. It provided a gain enhancement of, at most, 0.2 dB and no other advantage.

Freq, GHz	Azimuth	Min Gain, dB	Gain, dB 9°	Peak Gain, dB	Max Sidelobe, dB	Beamwidth	Efficiency, %
44	90°	29.0	--	34.3	23.7	2.57°	42.2
	70.9°	28.2	--	--	21.6	--	--
	60°	27.4	28.3	--	21.6	--	--
43	90°	29.5	--	34.47	20.3	2.46°	43.5
	60°	27.8	29.3	--	19.8	--	--
45	90°	29.0	--	34.55	23.7	2.34°	41.6
	60°	27.4	27.9	--	21.7	--	--

Table 7. Waveguide lens performance.

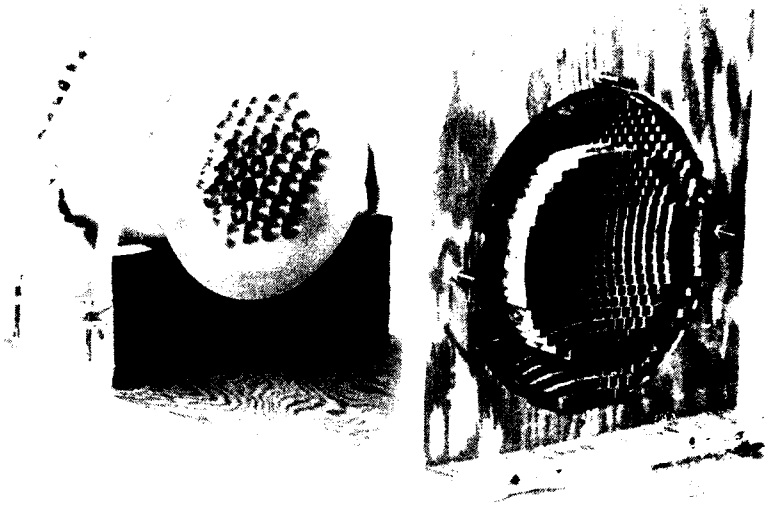

Figure 30a. Waveguide lens system front.

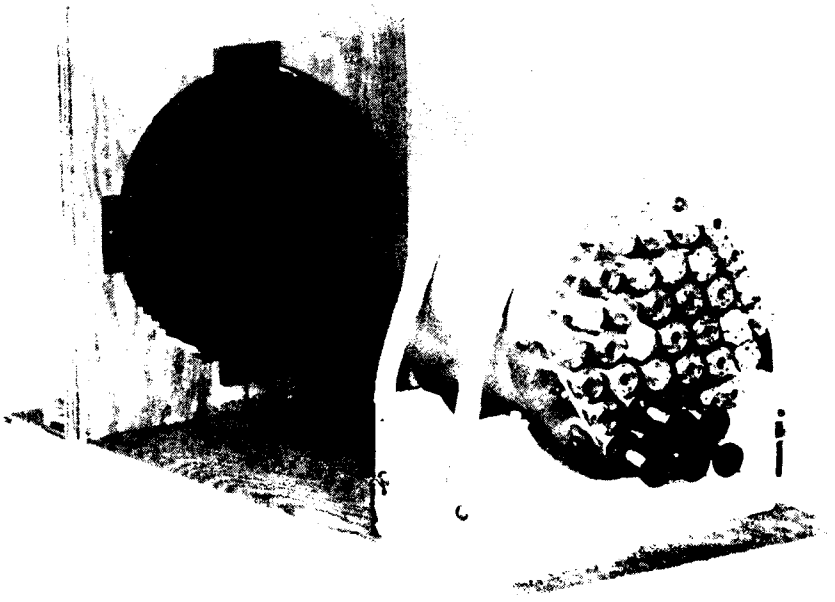

Figure 30b. Waveguide lens system rear.

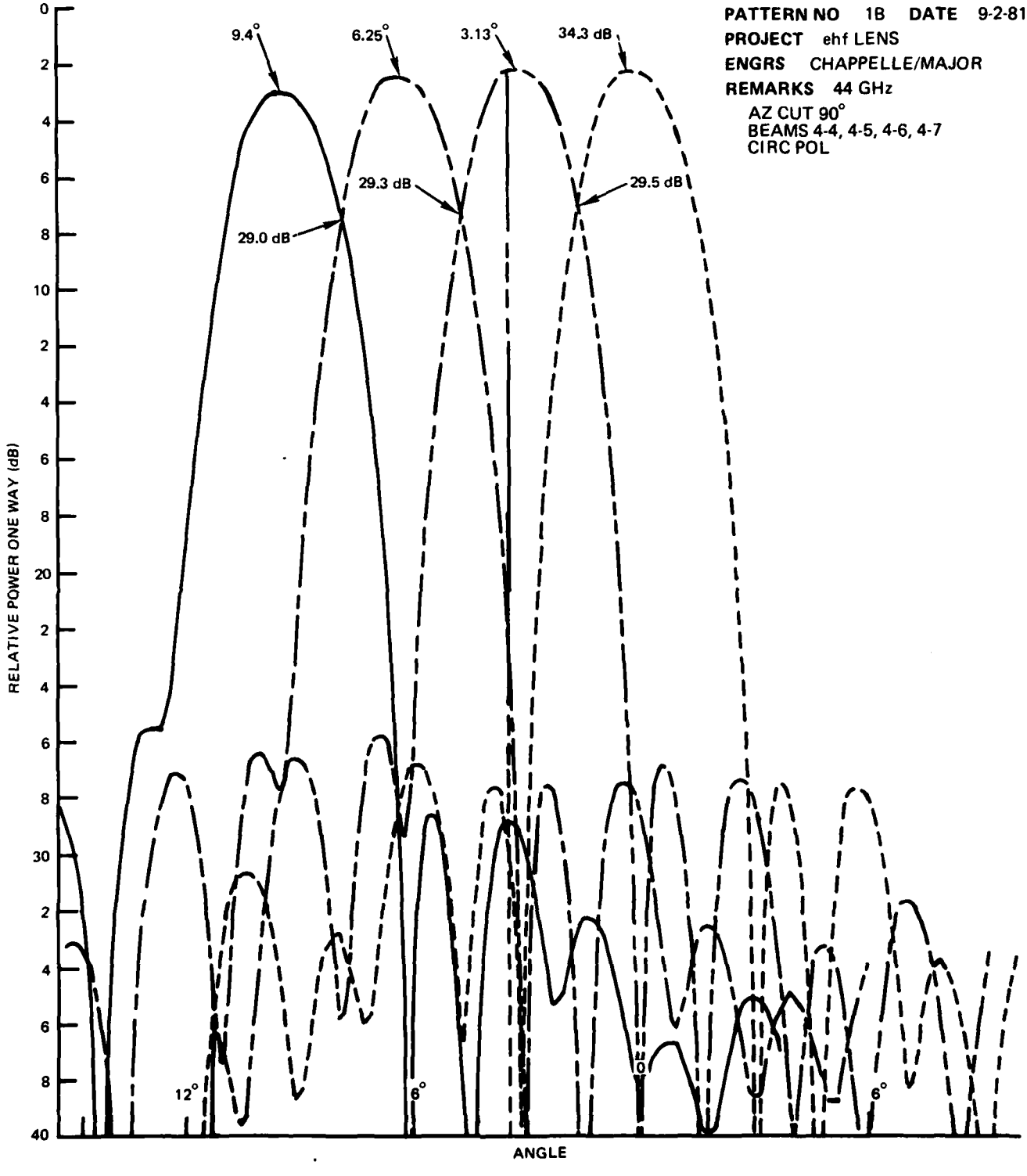

Figure 31a. Lens pattern (44 GHz, $\phi = 90°$.)

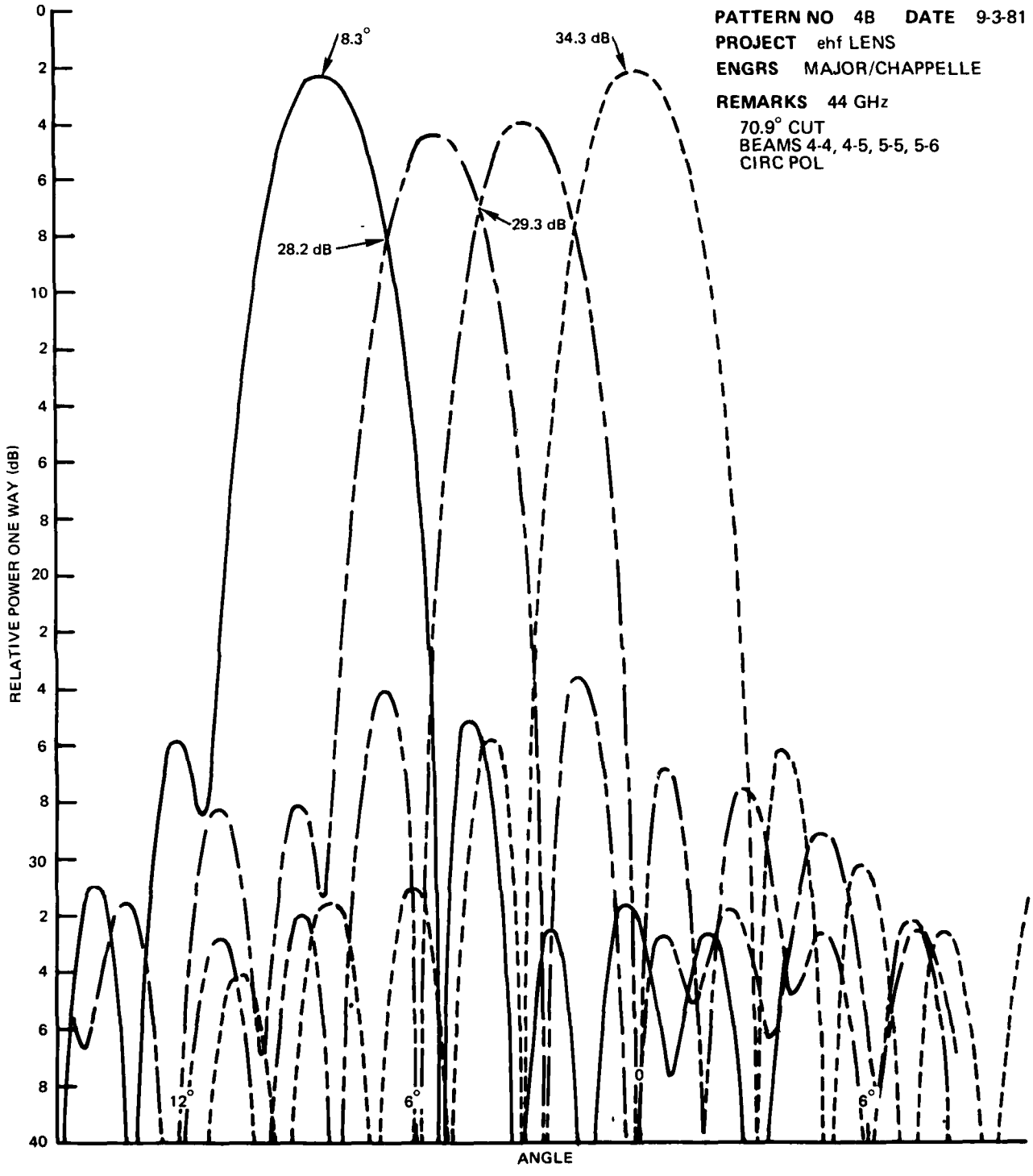

Figure 31b. Lens pattern. (44 GHz, $\phi = 70.9°$.)

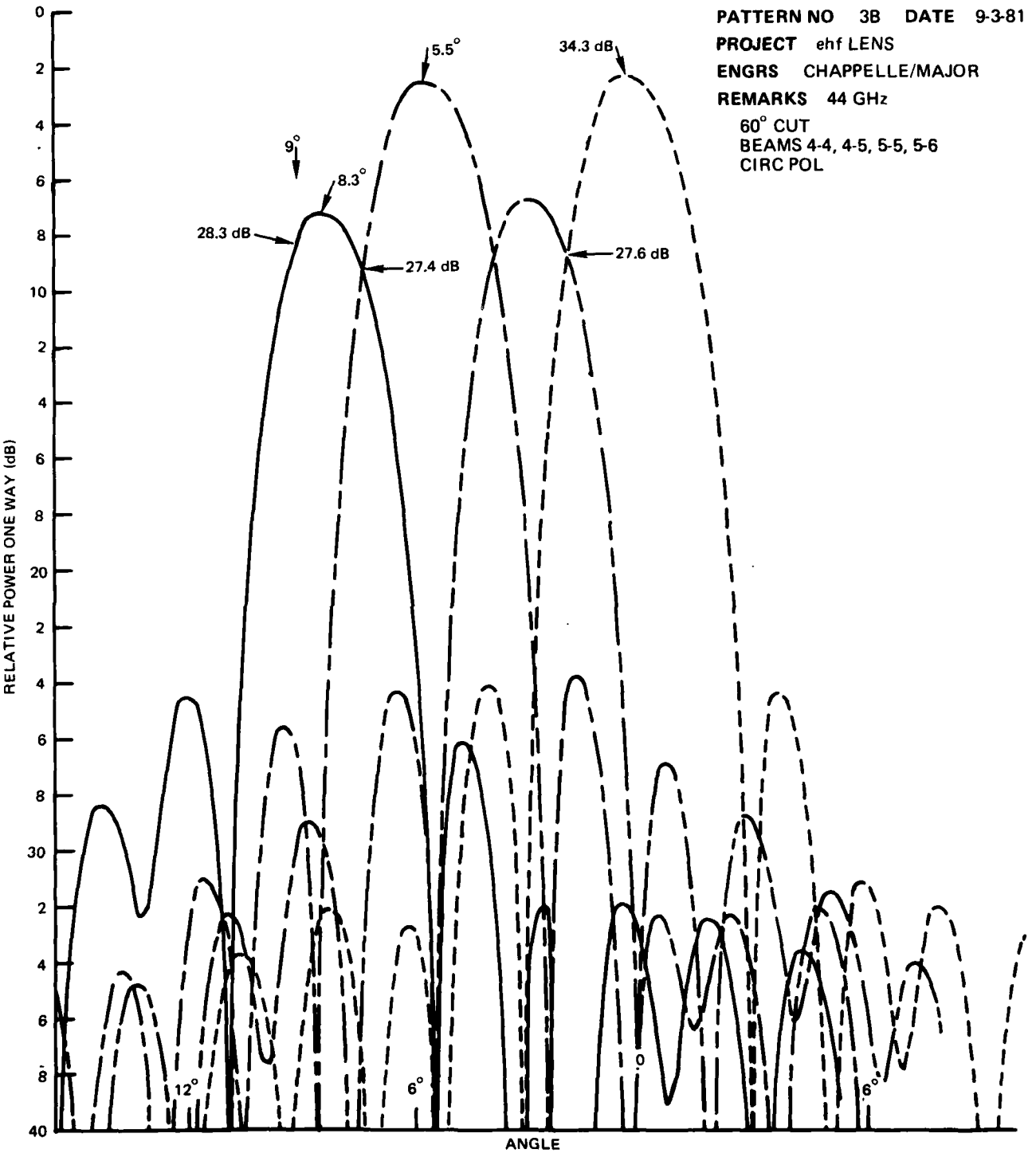

Figure 31c. Lens pattern. (44 GHz, $\phi = 60°$.)

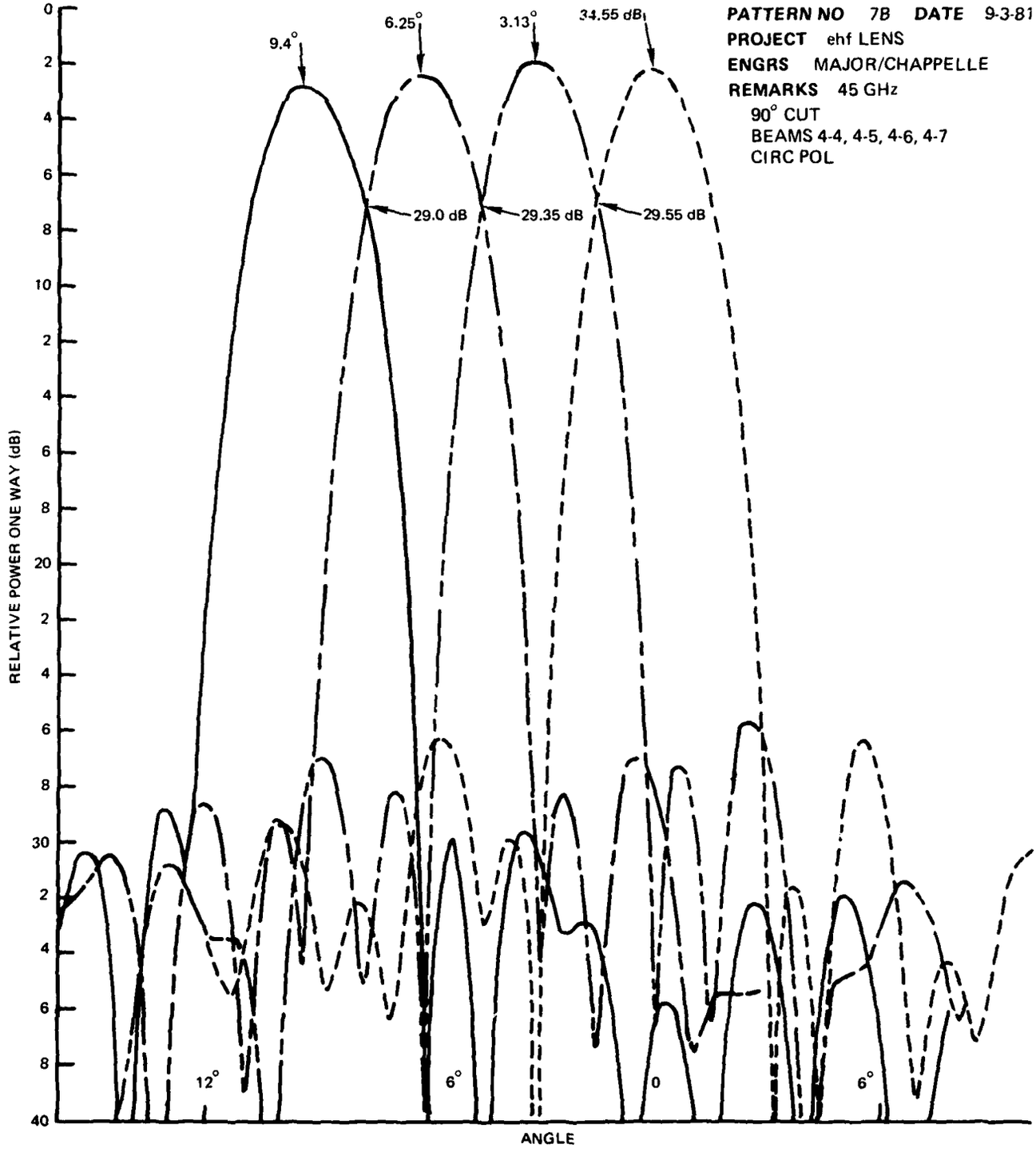

Figure 32a. Lens pattern. (45 GHz, $\phi = 90°$.)

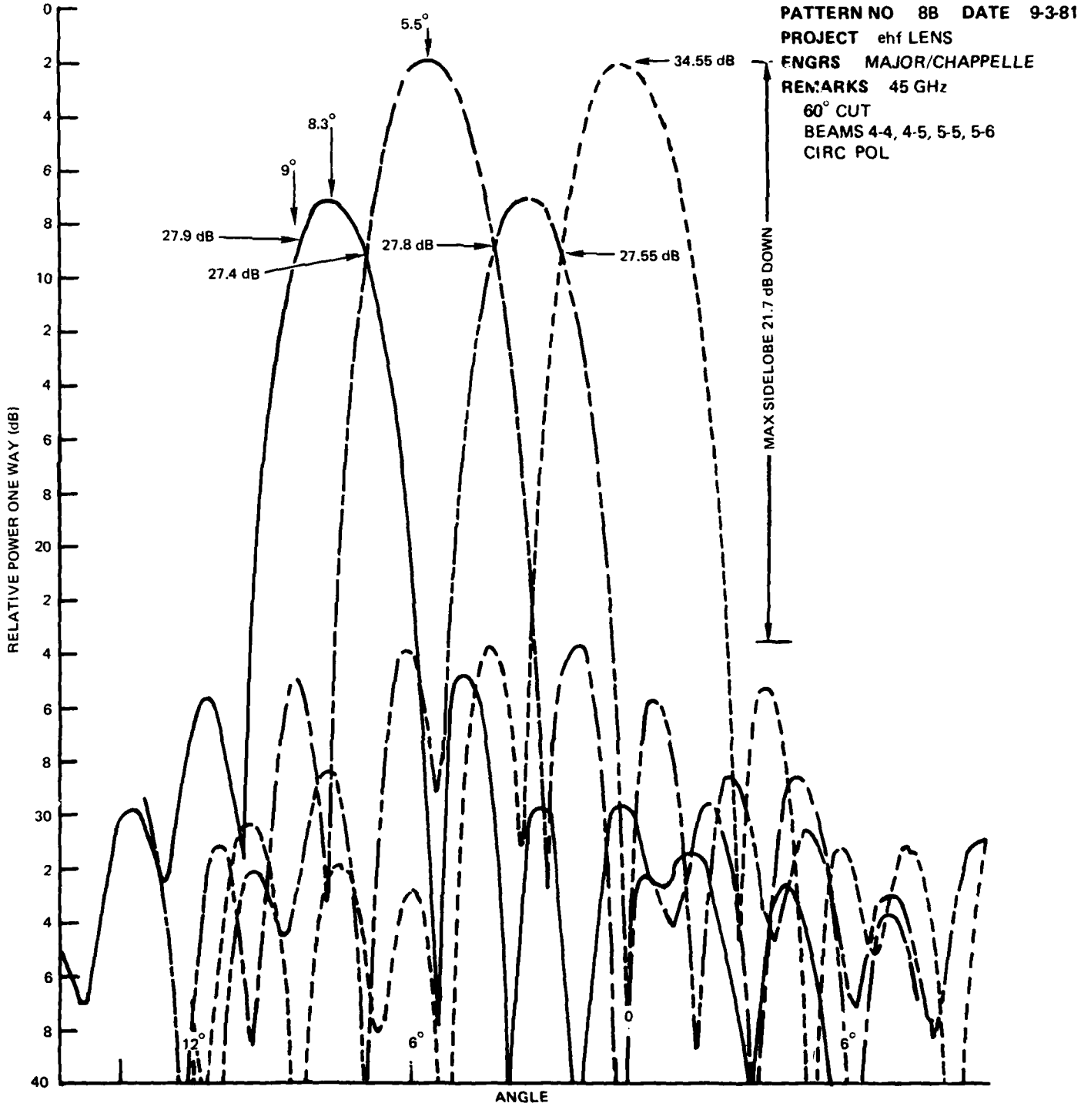

Figure 32b. Lens pattern. (45 GHz, $\phi = 60°$.)

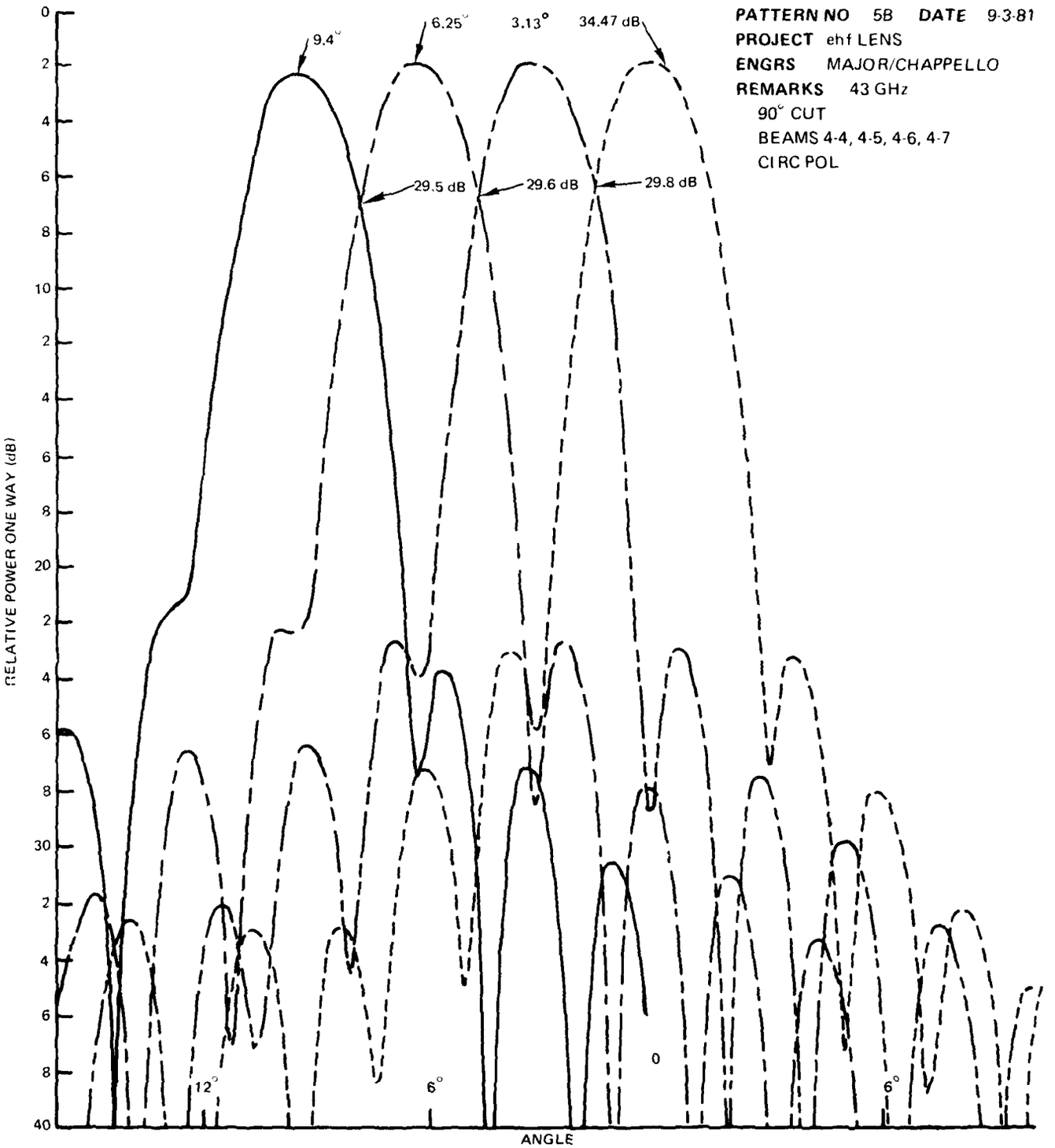

Figure 33a. Lens pattern. (43 GHz, $\phi = 90°$.)

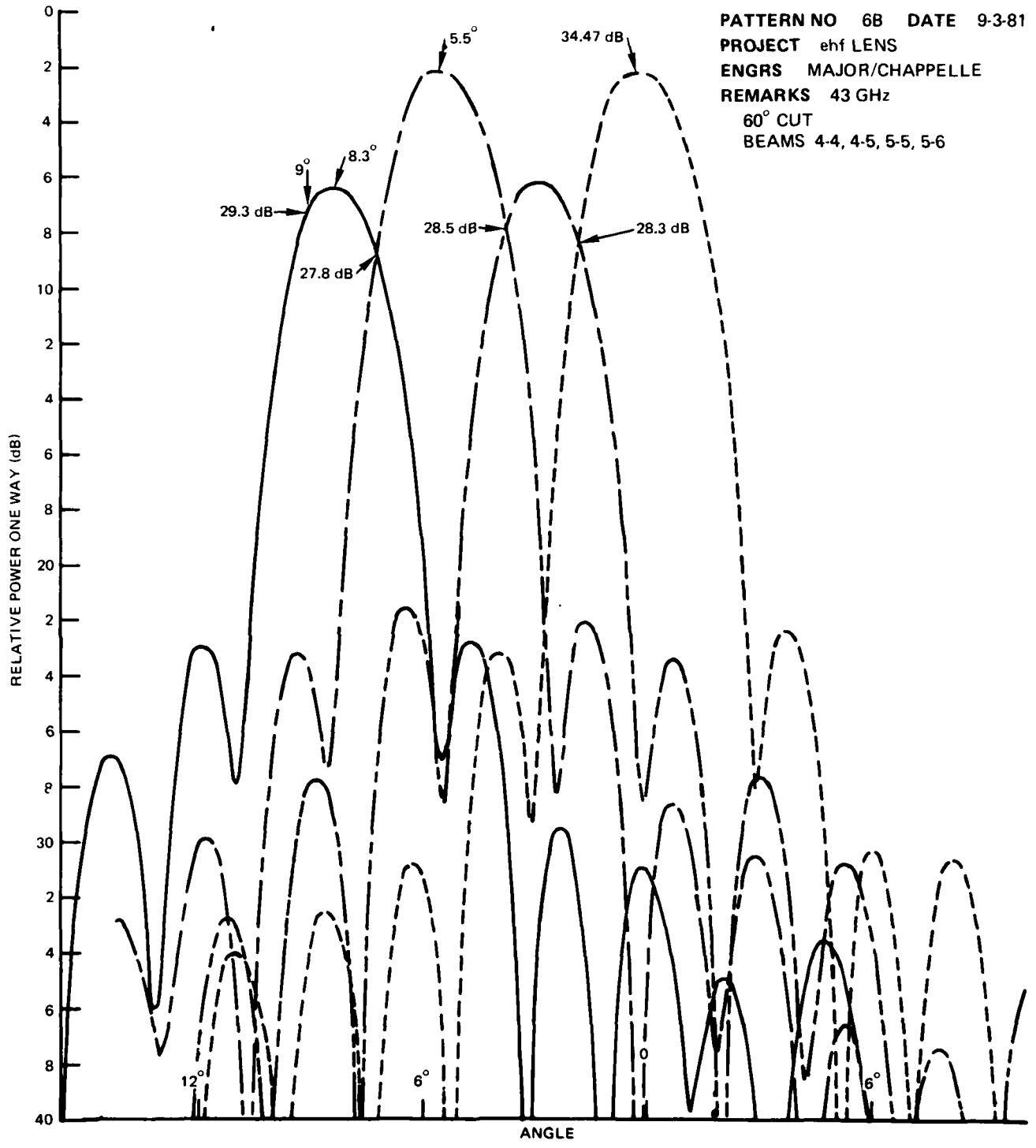

Figure 33b. Lens pattern. (43 GHz, $\phi = 60°$.)

5.4 SUMMARY

Table 8 compares the measured results of this lens system with the corresponding predicted/desired values. The waveguide lens system met or exceeded expectations on most points, and was close on all.

Component	Measured	Predicted/Desired
LENS:		
Freq	43-45 GHz	43-45 GHz
Beamwidth	2.34°-2.57°	$<3°$
G_{MIN}	27.4 dB	27 dB
Scan	$>17.3°$	17.3°
Sidelobe	$\geqslant$19.8 dB down	$>$20 dB down
η	$\geqslant$41.6%	$\geqslant$40%
Size	6.9"	$<10"$
HORN:		
Gain	15.35-15.85 dB	$>$15 dB
η	~79%	$>$73%
Isolation	$\geqslant$43 dB	$>$30 dB
POLARIZER:		
Axial ratio	$\leqslant$1.3 dB	$<$2 dB
MIXER:		
rf frequency	43-45 GHz	43-45 GHz
IF frequency	2-4 GHz	2-4 GHz
LC	9.6-8.8 dB at 2 mW 9.0-8.2 dB at 5 mW	9 to 8 dB at 2 mW
rf VSWR	$\leqslant$1.5:1	$<$2.0:1
IF VSWR	$\leqslant$2.1:1	$<$2.0:1
Degraded performance	5 dB typical, 6.2 dB max	6 dB max

Table 8. Waveguide lens system summary.

REFERENCES

1. Balanis, C.A., Dielectric Constant and Loss Tangent Measurement at 60 and 90 GHz Using the Fabry-Perot Interferometer, Microwave Journal, p 39-44, March 1971.
2. Saad, T.S., Microwave Engineer's Handbook, v 1, p 15, Artech House, Inc, 1971.

3a. MIT Lincoln Lab TN 1975-39, Optimization of a Communication Satellite Multiple Beam Antenna, by A.R. Dion, 17 May 1975.

3b. MIT Lincoln Lab TN 1979-33, Minimum Directive Gain of Hopped-Beam Antennas, by A.R. Dion, p 14, 11 June 1979.

4. Silver, S., Microwave Antenna Theory and Design, 1st ed, p 407 and 409, McGraw-Hill 1949.
5. Reynolds, J.F., and M.R. Rosenzweig, Learn the Language of Mixer Specifications, Microwaves, p 74 and 76, May 1978.
6. Anaren Catalog, p 159.

7. NOSC TN 550, MIC Millimeter-Wave Channelized Downconverter, by D. Rubin and D. Saul, p 13 and 15, 11 October 1978.

8. Levy, R., Directional Couplers, Advances in Microwaves, v 1, 1966.

9. Saleh, A.A.M., Planar Electrically Symmetric N-Way Hybrid Power Dividers/ Combiners, IEEE T-MTT-28, p 555-563, June 1980.

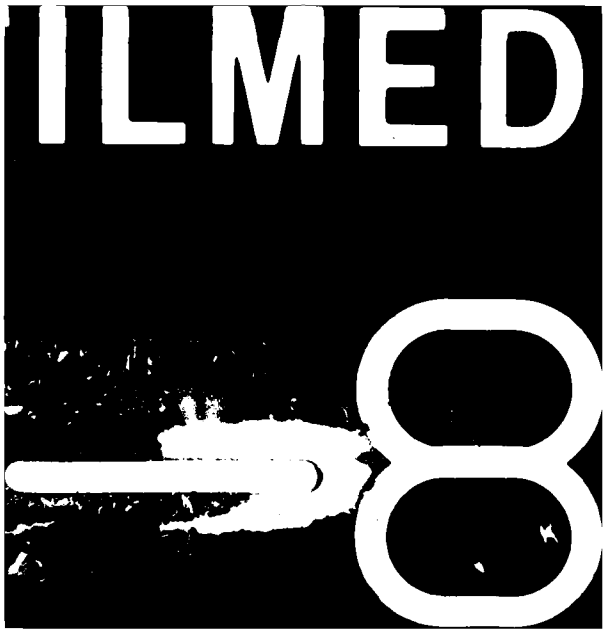
ILMED
8